



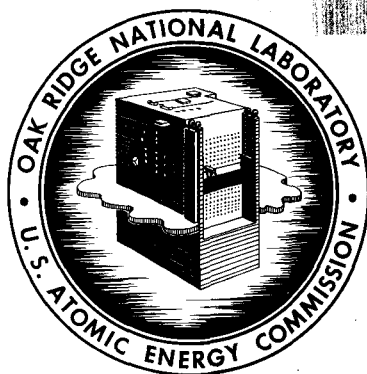
3 4456 0059779 9

GENERAL DOCUMENT LIBRARY  
DOCUMENT COLLECTION

ORNL-3039  
UC-4 - Chemistry  
TID-4500 (16th ed.)

REVIEW AND CORRELATION OF IN-PILE  
ZIRCALOY-2 CORROSION DATA AND A MODEL  
FOR THE EFFECT OF IRRADIATION

G. H. Jenks



**OAK RIDGE NATIONAL LABORATORY**

operated by

UNION CARBIDE CORPORATION

for the

U.S. ATOMIC ENERGY COMMISSION

**\$1.00**

Printed in USA. Price \_\_\_\_\_ . Available from the

Office of Technical Services  
Department of Commerce  
Washington 25, D. C.

**LEGAL NOTICE**

This report was prepared as an account of Government sponsored work. Neither the United States, nor the Commission, nor any person acting on behalf of the Commission:

- A. Makes any warranty or representation, expressed or implied, with respect to the accuracy, completeness, or usefulness of the information contained in this report, or that the use of any information, apparatus, method, or process disclosed in this report may not infringe privately owned rights; or
- B. Assumes any liabilities with respect to the use of, or for damages resulting from the use of any information, apparatus, method, or process disclosed in this report.

As used in the above, "person acting on behalf of the Commission" includes any employee or contractor of the Commission, or employee of such contractor, to the extent that such employee or contractor of the Commission, or employee of such contractor prepares, disseminates, or provides access to, any information pursuant to his employment or contract with the Commission, or his employment with such contractor.

ORNL-3039

Contract No. W-7405-eng-26

REACTOR CHEMISTRY DIVISION

REVIEW AND CORRELATION OF IN-PILE ZIRCALOY-2 CORROSION  
DATA AND A MODEL FOR THE EFFECT OF IRRADIATION

G. H. Jenks

DATE ISSUED

JUL - 6 1961

OAK RIDGE NATIONAL LABORATORY  
Oak Ridge, Tennessee  
operated by  
UNION CARBIDE CORPORATION  
for the  
U. S. ATOMIC ENERGY COMMISSION

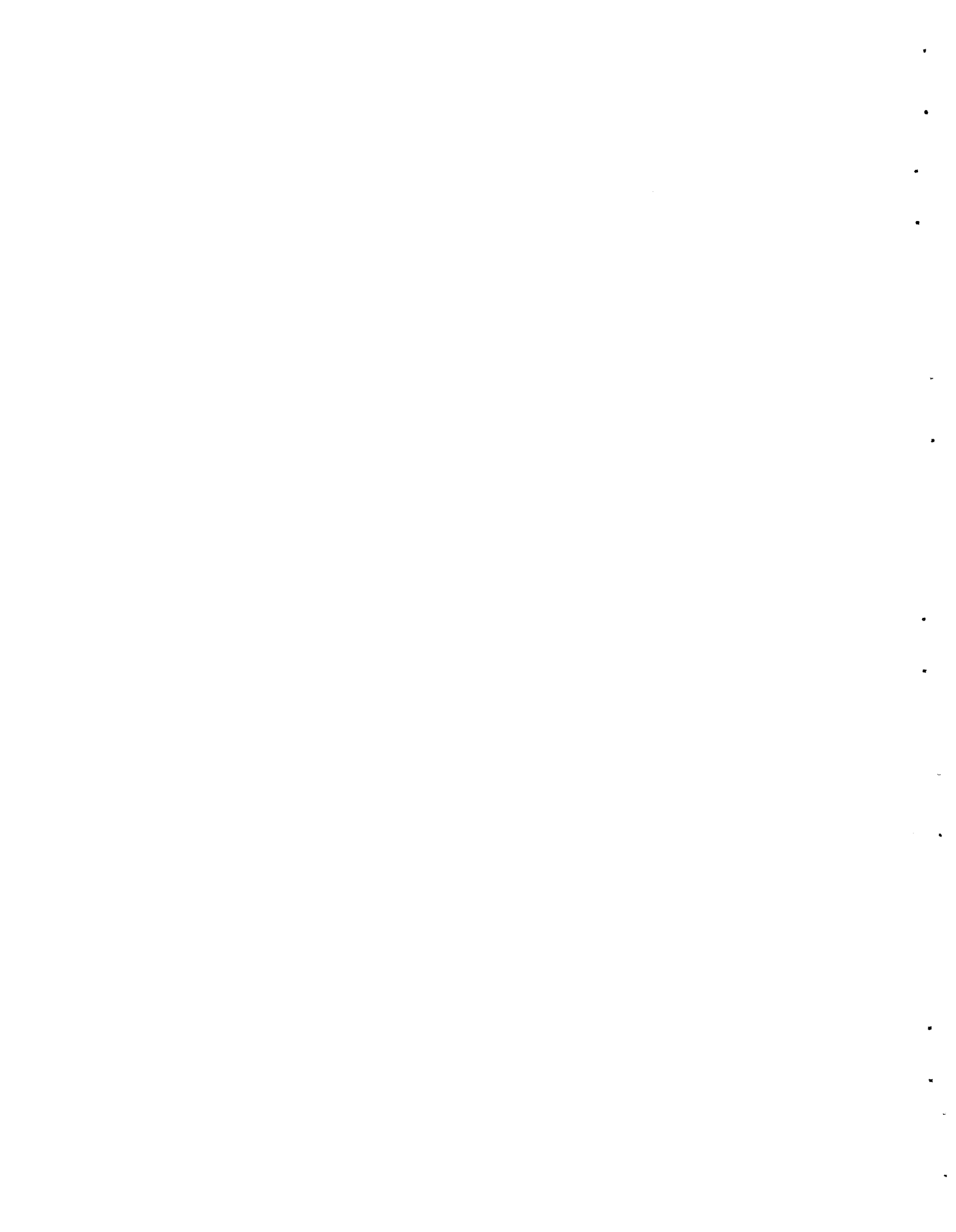


3 4456 0059779 9



## CONTENTS

ABSTRACT .....	1
1. INTRODUCTION .....	1
2. DERIVATION OF CORROSION-RATE EQUATION .....	3
2.1 Metal-Damage Model Assumed .....	4
2.2 Oxide Damage Models .....	9
3. REVIEW OF EVIDENCE FOR URANIUM SORPTION AND CONSIDERATION OF ITS EFFECT ON IRRADIATION INTENSITY .....	9
4. IN-PILE ZIRCALOY-2 CORROSION RESULTS .....	14
4.1 Applicability of Equation to Corrosion Data .....	15
Value of $K$ and $K_1$ at 280°C .....	15
Value of $K$ at 250°C .....	17
Value of $K$ at 300°C .....	18
Relationship Between $K$ and Temperature .....	18
Other Values of $K_1$ .....	20
4.2 Effect of Solution Velocity on Corrosion .....	23
Covered Surfaces of Channel Specimens .....	31
Graphical Interpretation of the Averages of Rates on Exposed and Covered Surfaces .....	31
Influence of Channel Angle .....	32
Discussion of Experimental Results for Velocity Effects on Corrosion .....	32
5. CONCLUSIONS .....	35
APPENDIX – Possible Significance of Temperature Independence of the Ratio $K_1/K$ .....	36



# REVIEW AND CORRELATION OF IN-PILE ZIRCALOY-2 CORROSION DATA AND A MODEL FOR THE EFFECT OF IRRADIATION

G. H. Jenks

## ABSTRACT

A review and a correlation of many of the data obtained at ORNL for the in-pile corrosion of Zircaloy-2 in uranyl sulfate solutions at elevated temperatures are presented. The correlation is based on the following equation for the relationship between the corrosion rate,  $R$ , and the fission power density in solution,  $P$ :  $1/R = K_1/KP^\alpha + 1/K$ , where  $\alpha$  is the factor by which the effective power density at the corroding surface is greater than that in the solution, because of uranium sorption on the surface, and  $K_1$  and  $K$  are constants which are evaluated from the experimental data.

A semiempirical model for the radiation effects on Zircaloy-2 corrosion which leads to this equation is described and discussed. In the model it is assumed that the major effects of radiation, in interaction with corrosion, are in the metal. However, the model is designed, in effect, to yield the equation, and other models in which the radiation corrosion results from damage to the protective oxide are not necessarily precluded.

The results of the correlation of the experimental data indicate that a general relationship between corrosion rate and solution power density of the form given by the above equation is obeyed within the power-density-range tested (up to 110 w/cc). The extrapolated value of  $K$  is essentially independent of solution composition but varies with temperature. The observed values are expressed fairly well by the equation  $K = 4.44 \times 10^{10} \exp(-22,900/RT)$ , where  $K$  has the units mpy (mils per year), and  $R$  in this case is the gas constant. The correlations further indicate that the value of the ratio  $K_1/K$  does not change appreciably with temperature and has the value of  $2.3 \text{ w cc}^{-1} \text{ mpy}^{-1}$  in the temperature range tested (225 to 330°C).

The value of  $\alpha$  prevailing during exposure depends upon the solution composition and the velocity of solution flow past the test surface. In some solutions the observed value of  $\alpha$  is unity even at low velocities. In others, notably those with low concentrations of uranium and other sulfate additives,  $\alpha$  values of 6 to 7 or more occur at low velocities. When  $\alpha$  values greater than unity occur at low velocities, the values at higher velocities are nearer unity and, under some flow conditions and in some solutions, are equal to unity. The observed  $\alpha$  values and the effects of velocity and solution composition are reasonably interpreted in terms of the amounts of uranium sorbed on nonprotective oxides near the specimen surface and the fractional contribution of this sorbed uranium to the total intensity of fission-recoil irradiation of the surface.

## 1. INTRODUCTION

Under simultaneous exposure of Zircaloy-2 to uranyl sulfate solutions at elevated temperatures and to reactor radiations, the Zircaloy-2 corrodes fairly uniformly at a rate which is approximately constant with time during irradiation and which is greater than the rate found in the absence of radiations. A considerable amount of information on the corrosion rate and other corrosion behavior under various experimental conditions is available from the results of a program of in-pile loop and autoclave studies at ORNL. This program also included experiments with fast-electron irradiations as well as nonradiation or laboratory-type experiments designed to help elucidate the mechanism of

the corrosion effects observed in-pile. Most of the results of this program have been reported previously,<sup>1-4</sup> but, for convenience, some of the general aspects of the results and the interpretations which provide background information for the following discussions are listed here.

1. With other conditions constant, the corrosion rate increases with increasing fission power density in solution but tends to level off at high power densities.

2. From the results of the fast-electron irradiation experiments together with those of the in-pile experiments, it has been concluded that the radiation effects on Zircaloy-2 corrosion are associated with changes in the metal or the protective oxide which are induced by heavy-nuclear-particle bombardment, that is, by fission-fragment recoils or by fast neutrons. In solutions containing fissionable uranium, the in-pile corrosion is due primarily to fission-fragment recoils.

3. Specimens exposed in-pile lose weight but retain a thin-appearing adherent film which frequently exhibits interference colors. Specimens removed from all-Zircaloy-2 autoclaves (all internal surfaces of autoclaves exposed to fission fragments) are usually covered with a brass-colored scale. This scale can be removed by drying and brushing to expose the thin-appearing film. Specimens exposed to fissioning solution in loop cores do not retain the brass-colored scale, and there is clear evidence that  $ZrO_2$  is deposited in portions of the loops which are not exposed to fissioning solution. The amount of zirconium found dissolved or suspended in the in-pile test solution is greater than that found out-of-pile.

The actual thickness of the thin-appearing film has not been determined in ORNL work, but as judged from comparison between the appearance of this film and those formed during out-of-pile corrosion, and from the near agreement between data for the amount of oxygen consumed in corrosion and that for specimen weight loss due to corrosion, the maximum thickness is probably less than 10,000 Å. Cox and co-workers<sup>5</sup> at Harwell have measured the weight and examined the surfaces of specimens exposed to low fission power densities (approximately 0.07 w/ml and less). They found that specimens increased in weight following the initiation of exposure until a total of several tenths of a milligram per square centimeter was reached. The total weight then started to decrease. Electron-microscope examination showed cracking in the oxide at weight gains of about 0.25 mg/cm<sup>2</sup> (corresponding to a film thickness of about 15,000 Å). Prior to this weight gain, there was no evidence of cracking or loss of adherency in the oxide, although unusual ridges were observed. The rate of corrosion during the period prior to cracking was greater than that prevailing out-of-pile at similar weight gains.

---

<sup>1</sup>G. H. Jenks, *Effects of Irradiation on the Corrosion of Zircaloy-2*, ORNL CF-57-9-11 (Sept. 39, 1957).

<sup>2</sup>G. H. Jenks, "Radiation Induced Corrosion of Zircaloy-2 and Zirconium," pp 232-45 in *Fluid Fuel Reactors* (ed. by J. A. Lane, H. G. MacPherson, and Frank Maslan), Addison-Wesley, Reading, Mass., 1958. References to all work carried out at ORNL prior to 1958 are included.

<sup>3</sup>R. J. Davis, *Tabular Summary of Zircaloy-2 In-Pile Rocking Autoclave Corrosion Data*, ORNL CF-58-6-92 (June 18, 1958).

<sup>4</sup>R. J. Davis, *Tabular Summary of In-Pile Autoclave Solution Corrosion Data*, ORNL CF-59-9-75 (Sept. 24, 1959).

<sup>5</sup>B. Cox, K. Alcock, and F. W. Derrick, *The Oxidation and Corrosion of Zirconium and Its Alloys*, AERE-R2932 (August 1959).

4. Uranium is found on the surface and in the scales, when present, of specimens exposed in most uranyl sulfate solutions. The amounts found are frequently sufficient to contribute appreciably to the intensity of fission-recoil irradiation of the surface.

The correlations and the interpretations of the in-pile corrosion data reported in the past<sup>1,2</sup> were based on a postulated model for the corrosion effects in which defects in the oxide lead to a loss of protective oxide and thus to thin films and correspondingly high rates. The assumed relationships between defect concentrations and corrosion rate and for the production and annealing of defects led to an equation of the general form of Eq. (1) for the relationship between the corrosion rate,  $R$ , and the fission power density in solution,  $P$ :

$$R = EP[1 - \exp(-L/R^{1.5})], \quad (1)$$

where  $E$  and  $L$  are constants for a given temperature and solution. This equation with the constants  $E$  and  $L$  evaluated from the experimental data satisfactorily expressed many of the corrosion-rate-power-density relationships observed under a given set of experimental conditions. It has proved useful in correlating and evaluating in-pile data with respect to the effects of variables such as temperature, solution composition, and changes in effective power density due to uranium sorption on a specimen surface.

More recent considerations of other possible models for the radiation effects have led to the formulation of a model which leads to Eq. (2) for the corrosion-rate-power-density relationship:

$$1/R = K_1/KP^\alpha + 1/K, \quad (2)$$

where for a given material,  $K$  is a constant for a given temperature and solution,  $K_1$  is a constant for a given temperature, and  $\alpha$  is the factor by which the effective power density is greater than the solution power density due to uranium sorption near or on the corroding surface. The term  $\alpha$  in Eq. (2) does not result from peculiarities of the model but, instead, from general considerations of the probable effects of sorbed uranium. The term can also be included in Eq. (1).

Equation (2) satisfactorily expresses the corrosion-rate-power-density relationships in many of the in-pile experiments. The form of the equation is such that straight-line plots of the data may be made, and the correlation and the interpretation of the data are more readily and probably more significantly accomplished than with Eq. (1).

## 2. DERIVATION OF CORROSION-RATE EQUATION

The model from which Eq. (2) was originally derived is one in which the major effects of radiation, in interaction with corrosion, are in the metal. Subsequent considerations of the possibilities that an equation of similar form could be derived from an oxide damage model have revealed no simple model which leads to this equation.

In the following sections, the metal-damage model is described and discussed in some detail to demonstrate that an apparently reasonable basis exists for the equation. A brief description will also be presented of the considerations which have been given to a model based on the mechanism

proposed by Cox *et al.*,<sup>5</sup> in which the tracks of fission recoils in the oxide comprise easy diffusion paths and thus account for radiation-induced corrosion. No attempt will be made to consider all available evidence for or against a particular mechanism. A brief review of several of the proposed general mechanisms which involve radiation damage in the oxide is given in the paper by Cox *et al.*<sup>5</sup>

## 2.1 METAL-DAMAGE MODEL ASSUMED

The postulates which comprise the model are the following:

1. The corrosion rate is directly proportional to the concentration of radiation defects in the metal near the oxide interface, and the loss of oxide and/or the changes in the oxide under irradiation have a negligible effect on the rate. That is,

$$R = aN, \quad (3)$$

where  $R$  is the corrosion rate,  $N$  is the concentration of radiation defects, and  $a$  is a constant. The reasonableness of these assumptions will be discussed later.

2. Radiation defects are formed at a rate directly proportional to the radiation intensity and are removed by radiation annealing, or, what is formally the same, the defect formation rate decreases as the concentration of radiation defects increases. The defects are also removed at a rate directly proportional to the defect concentration by some process which may be construed as thermal or, possibly, corrosion annealing. It will be assumed in the development of the model that this process is thermal annealing. The possibility that the process is corrosion annealing will be discussed in the Appendix. These postulates can be expressed as

$$dN/dt = K''P\alpha - K^0P\alpha N - K'N, \quad (4)$$

where  $K''$  and  $K^0$  are constants associated, respectively, with the production and radiation annealing of radiation defects,  $P\alpha$  is the effective power density, and  $K'$  is a thermal-annealing constant.

The author is unaware of any direct evidence for radiation annealing of radiation damage in metals at elevated temperatures. However, experimental evidence has been reported by Cooper, Koehler, and Marx<sup>6</sup> for radiation annealing in metals (silver, copper, and gold) under deuteron bombardment at very low temperatures, where thermal annealing did not occur. Their expression for the differential production and annealing of lattice defects which was proposed and which accounted for the experimental data was of the same general form as that given by the first three terms in Eq. (4). Also, Brinkman<sup>7</sup> has suggested from theoretical considerations that thermal spikes of sufficiently high energy are capable of annealing interstitial-vacancy pairs, and Brinkman and Gilbert<sup>8</sup> have reported experimental evidence for such annealing by fission recoils in thorium metal.

---

<sup>6</sup>H. G. Cooper, J. S. Koehler, and J. W. Marx, *Phys. Rev.* **97**, 599 (1955).

<sup>7</sup>J. A. Brinkman, *On the Nature of Radiation Damage in Metals*, NAA-SR-198 (Dec. 22, 1952).

<sup>8</sup>J. A. Brinkman and W. S. Gilbert, *Effects of Fission Fragments on Radiation Damaged Metal*, NAA-SR-262 (July 31, 1953).

Thermal annealing of radiation damage in zirconium occurs at the temperatures under consideration, but at least for some types of damage the annealing is at fairly low rates. Kemper and Kelley<sup>9</sup> irradiated zirconium at 50 to 60°C to integrated fluxes of  $5.7 \times 10^{19}$  to  $2.4 \times 10^{20}$  *mt*, thermal, in a Hanford reactor and subsequently heated the specimens at temperatures in the range 250 to 350°C. At 250°C, approximately 18% of the radiation-induced increase in yield strength annealed in 100 hr, and at 300°C about 40% was removed in the same period of time. At 350°C about 75% was removed in 160 hr.

3. The defect concentration reaches a steady state with respect to formation and annealing of defects; that is, the time of irradiation has no limiting effect on the steady-state defect concentration under all conditions tested. At steady state, Eq. (4) becomes

$$N_s = \frac{K''Pa}{K' + K^0Pa} \quad (5)$$

Substitution of Eq. (5) into Eq. (3) yields

$$R_s = \frac{aK''Pa}{K' + K^0Pa} \quad (6)$$

This equation may be rewritten in the form of Eq. (2) with new constants as defined in Eqs. (7) and (8):

$$1/R_s = K_1/KPa + 1/K, \quad (7)$$

$$K = aK''/K^0,$$

$$K_1 = K'/K^0. \quad (8)$$

The term  $K_1$  thus defined is the ratio of a thermal-annealing constant and a radiation-annealing constant and as such would not be expected to change in value with solution composition, but would be expected to change with temperature due to a change in the value of  $K'$ . The terms  $K''$  and  $K^0$  in Eq. (7) would not be expected to change appreciably with temperature or solution composition, but the term  $a$  would be expected to change with temperature and possibly with solution composition. Terms for the nonradiation corrosion are neglected in this development, since such corrosion in the usual in-pile test is negligible.

The possibility that radiation-produced changes in the Zircaloy-2 near the metal-oxide interface comprise the major source of radiation-induced corrosion has not been seriously considered previously. However, it is well known that the corrosion resistance of zirconium in high-temperature water without radiation is markedly affected by machining or abrading of the surface, and that the

---

<sup>9</sup>R. S. Kemper, Jr., and W. S. Kelley, *ASTM Proc.* 56, 823 (1956).

best corrosion resistance is obtained with an undisturbed, chemically polished surface.<sup>10,11</sup> Disturbed surface layers apparently affect Zircaloy-2 corrosion also but to a lesser extent. Also, different heat treatments have different effects on the Zircaloy-2 corrosion. Irradiation by fast neutrons is known to effect substantial changes in the ductility and the ultimate and yield strength of Zircaloy-2 at temperatures in the range under consideration as well as at lower temperatures.<sup>11</sup> Changes in hardness and creep properties also occur.<sup>11</sup> It thus appears possible that changes in the metal under heavy-particle irradiation may affect the corrosion adversely. As additional support for the concept that radiation damage in the metal affects corrosion adversely, it may be noted that Carpenter *et al.*<sup>12</sup> have recently reported that the gaseous oxidation of copper at 150°C was increased as a result of prior exposure to reactor radiations. The enhanced reactivity appeared to be strongest in the thin-film region up to about 700 Å. They suggest that the increased reactivity is attributable to crystal-defect structures. They also obtained indications that the rate of dissolution of copper in  $\frac{1}{3}$  M Fe(NO<sub>3</sub>)<sub>3</sub> solutions at 5°C is increased by prior exposure of the copper to reactor radiations.

The formal bases for postulating that the corrosion rate of the metal increases in direct proportion to the concentration of radiation defects in the metal and that the observed losses and/or changes in the oxide under irradiation have little effect on the rate are expressed in Eqs. (9) and (10) for the relationship between corrosion rate and protective-oxide thickness out of radiation, and for the kinetics of protective-oxide formation, also out of radiation:

$$dx'/dt = Ae^{-Bx} , \quad (9)$$

$$dx/dt = Ae^{-Bx} - CA/B , \quad (10)$$

where  $x'$  is the total oxide formed at time  $t$ ,  $x$  is the thickness of protective oxide, and  $A$ ,  $B$ , and  $C$  are constants for a given experimental system and temperature. As will be discussed below,  $C$  may be independent of temperature. These equations imply that the corrosion of Zircaloy-2 proceeds according to the well-known logarithmic rate law but that, in effect at least, the protective oxide changes to nonprotective at a rate given by  $CA/B$ .

As will be described in detail elsewhere,<sup>13</sup> these equations were postulated from the results of an analysis of some of the published data for (1) zirconium and Zircaloy-2 weight gains in oxygen at temperatures in the range 275 to 600°C and during exposure times up to 6 hr;<sup>14-16</sup> (2) Zircaloy-2

<sup>10</sup>D. E. Thomas, "Corrosion in Water and Steam," pp 608-40 in *Metallurgy of Zirconium* (ed. by Benjamin Lustman and Frank Kerze, Jr.), McGraw-Hill, New York, 1955.

<sup>11</sup>G. E. Zima, *A Review of the Properties of Zircaloy-2*, HW-60908 (Oct. 14, 1959).

<sup>12</sup>F. D. Carpenter *et al.*, *Irradiation Effects on the Surface Reactions of Metals, Summary Report Oct. 1, 1958 to Nov. 1, 1959*, GA-1093.

<sup>13</sup>G. H. Jenks, report in preparation.

<sup>14</sup>E. A. Gulbransen and K. F. Andrew, *Trans. Am. Inst. Mining Met. Petrol. Engrs.* **185**, 515 (1949); *J. Metals*, August 1949.

<sup>15</sup>E. A. Gulbransen and K. F. Andrew, *Trans. Am. Inst. Mining Met. Petrol. Engrs.* **209**, 394 (1957); *J. Metals*, April 1957.

<sup>16</sup>E. A. Gulbransen and K. F. Andrew, *Trans. Am. Inst. Mining Met. Petrol. Engrs.* **212**, 281 (1958); *Trans. Met. Soc. AIME*, April 1958.

weight gains in oxygen and steam at 400°C during exposure times up to several hundred days;<sup>17</sup> (3) Zircaloy-2 corrosion in uranyl sulfate solutions at 250 and 290°C determined at ORNL by oxygen-consumption measurements in autoclave-type experiments during exposure periods of about 50 days.<sup>18</sup> It was found that for a given material the short-time oxidation data examined, principally those of Gulbransen and Andrew,<sup>14-16</sup> can be expressed reasonably well by equations of the above forms with values of  $A$  and  $1/B$  which increase regularly with increasing temperature and with  $C$  approximately independent of temperature. The long-term weight-gain data for Zircaloy-2 in oxygen and steam can be expressed fairly well by the same equations and with values for the constants determined for the 6-hr, 400°C data of Gulbransen and Andrew. The uranyl sulfate corrosion data can also be expressed by equations of the same general form, although for the few data available no definite relationship between the values for the protective-oxide decay terms and of  $A$  and  $B$  could be established, and the values of  $A$  were not accurately determined. The values of  $B$  were about a factor of 10 less than those obtained by extrapolation of the  $B$  values determined from the oxygen data of Gulbransen and Andrew.

It has also been found that the data for the weight gain of Zircaloy-2 in deaerated water at 320°C obtained by Britton and Wanklyn and corrected by Flint<sup>19</sup> for weight loss due to dissolution of  $ZrO_2$  in the water are expressed reasonably well by Eqs. (9) and (10) with a value of  $B$  which is in line with that found for the  $UO_2SO_4$  solutions, a value of  $A$  about equal to that obtained by extrapolation of the values for the oxygen data of Gulbransen and Andrew, and a value of  $C$  about the same as that found for the Gulbransen and Andrew data.

Since the time this work was initiated, Cox<sup>20</sup> has also suggested that logarithmic kinetics are obeyed in the aqueous corrosion of zirconium and Zircaloy-2, although he suggests that the weight-gain data prior to breakaway are explained on the basis that two different mechanisms are operative.

Bacarella<sup>21</sup> has also found evidence that the logarithmic rate law is followed over periods of several days in the high-temperature corrosion of Zircaloy-2 in oxygenated 0.05  $m$   $H_2SO_4$ .

If logarithmic kinetics are indeed obeyed in the growth of protective oxide films on Zircaloy-2 during aqueous corrosion, it appears reasonable to postulate that the reactivity or structure of the metal has a direct effect on the corrosion rate for a given oxide thickness. This follows from the consideration that the factor  $A$  in Eq. (9) or (10) is numerically equal to the corrosion rate in the absence of a sensible amount of protective oxide and thus may be regarded as a measure of the rate at which corrosion processes can occur near the metal-oxide interface. A similar interpretation of the factor  $A$  is apparently assumed by Evans in the easy-diffusion path or pore mechanism which he

---

<sup>17</sup>D. E. Thomas and S. Kass, *J. Elec. Soc.* **104**, 261 (1957).

<sup>18</sup>G. H. Jenks *et al.*, *HRP Quart. Progr. Rept. Oct. 31, 1954*, ORNL-1813, pp 81-82.

<sup>19</sup>O. Flint, *Corrosion* **16**, 229t (1960).

<sup>20</sup>B. Cox, *The Oxidation and Corrosion of Zirconium and Its Alloys*, AERE-R2931 (May 1959).

<sup>21</sup>A. L. Bacarella, *HRP Quart. Progr. Rept. Oct. 31, 1959*, ORNL-2879, pp 148-52.

has proposed to explain logarithmic kinetics in the growth of oxide films.<sup>22-24</sup> In the Evans mechanism, the rate of reaction is proportional to the number of pores per unit area and is independent of thickness of the film except that the number of pores changes with film thickness. The rate for a given number of pores is limited by the rate at which the metal in contact with the pores can react or by the rate at which diffusion can occur across a thin oxide film of nearly constant thickness near the metal-oxide interface.

In effect, then, it is assumed in the model that the fission-recoil irradiation increases the value of  $A$  by increasing the reactivity of the metal near the metal-oxide interface or by decreasing the protective qualities of a very thin film of nearly constant thickness near the metal-oxide interface. If the validity of Eq. (10) is assumed, an increase in the value of  $A$  results in a proportionate increase in the value of the steady-state corrosion rate as assumed in the model.

The mechanism by which decay of the protective oxide occurs to give rise to the term  $CA/B$  in Eq. (10) is unknown. However, it may be speculated that the process is one which includes a transformation of some of the underlying protective oxide to an adherent surface layer of nonprotective oxide, that is, an oxide through which the rate of transfer of reagents is large compared with the rate through the protective material. Evidence for a transformation in the structure of the oxides formed on zirconium and zirconium-tin alloys during water corrosion at 315°C has been presented by Schwartz, Vaughan, and Cocks.<sup>25</sup> They found that the initial film had a tetragonal structure, while after about 4 hr exposure, monoclinic oxide was present over the surface or in spots on the oxide. Also, in the aqueous corrosion of zirconium and Zr-2.5% Sn at 315°C, Misch<sup>26</sup> has found that the film thicknesses indicated by capacitance measurements deviated from those measured by optical methods after short exposure times and before the breakaway thickness was reached. It was suggested that as the oxides grew, they developed a permeability, perhaps by cracking, to the electrolyte in which the capacitances were measured.

If it is assumed that an appreciable fraction of the oxide present on Zircaloy-2 is indeed nonprotective as suggested above, then loss of oxide such as occurs under irradiation may have little effect on the corrosion unless the relatively thin underlying protective oxide is also removed. Similarly, it is possible that changes which are observed in the oxide under irradiation may be present only in the relatively heavy nonprotective oxide and not in the thinner protective oxide.

---

<sup>22</sup>U. R. Evans, *Metallic Corrosion Passivity and Protection*, pp 135-37, Longmans, Green, New York, 1948.

<sup>23</sup>D. E. Davies, U. R. Evans, and J. N. Agar, *Proc. Roy. Soc.* **225A**, 443 (1954).

<sup>24</sup>U. R. Evans, *The Corrosion and Oxidation of Metals*, pp 833-36, Edward Arnold, London, 1960.

<sup>25</sup>C. M. Schwartz, D. A. Vaughan, and G. G. Cocks, *Identification and Growth of Oxide Films on Zirconium in High-Temperature Water*, BMI-793 (Dec. 17, 1952).

<sup>26</sup>R. D. Misch, *Characteristics of Anodic and Corrosion Films on Zirconium*, ANL-6149 (May 1960).

## 2.2 OXIDE DAMAGE MODELS

As a result of investigations of Zircaloy-2 corrosion in and out of radiation, Cox *et al.*<sup>27</sup> proposed a mechanism to explain radiation corrosion in which fission tracks in the oxide provide easy diffusion paths for transfer of reactive species. The oxide breaks down at some thickness because of stresses set up by nonuniform growth through the easy paths. This mechanism of growth and failure of the oxide is similar to that suggested<sup>20</sup> for out-of-radiation corrosion, where diffusion also occurs through preferred paths, for example, through paths at grain boundaries. This mechanism is not precluded as one which would give rise to a relationship of the form of Eq. (2). However, the author has been unable to visualize a simple, satisfactory model employing this mechanism which leads to the equation – primarily because it appears likely that corrosion annealing of the fission tracks would be an important factor, and such annealing is expected to proceed at a rate proportional to the square of the number of tracks.<sup>23,24</sup>

Consideration of other suggested mechanisms in which the radiation effects are in the oxide has revealed no simple model which leads to an equation of the form of Eq. (2).

## 3. REVIEW OF EVIDENCE FOR URANIUM SORPTION AND CONSIDERATION OF ITS EFFECT ON IRRADIATION INTENSITY

Uranium is found in the heavy scales which coat Zircaloy-2 specimens recovered after in-pile exposure in uranyl sulfate solutions in autoclaves. Uranium has also been found on the surface of these specimens after the heavy scales have been removed by drying and brushing to expose the thin-appearing adhering film, and on the surfaces of specimens recovered after exposure in some solutions in loop cores. The latter specimens are also covered with thin-appearing adhering films but are free of heavy scale of the type found in autoclaves.

Most of the heavy scales recovered from autoclave experiments have been analyzed for uranium content. The results obtained in a number of experiments are listed in Table 1. Corrosion results obtained in many of these experiments are considered in Sec 4, and for this purpose some experiments are listed for which uranium data are not available. These autoclave data and references to the original reports are given in refs 28 and 29.

As may be seen in the table, the uranium found in scales exposed in solutions of 0.17 *m* UO<sub>2</sub>SO<sub>4</sub> containing 0.04 *m* or zero excess H<sub>2</sub>SO<sub>4</sub> ranged from about 1 to 10 wt %, and, with only one exception, the scales from solutions with the added acid contained less uranium than those from zero-acid solutions. The addition of 0.45 *m* H<sub>2</sub>SO<sub>4</sub> in one experiment appeared to eliminate uranium from the scale. The uranium content of the scales obtained in experiments with 1.3 *m* UO<sub>2</sub>SO<sub>4</sub> was about

---

<sup>27</sup>B. Cox, K. Alcock, and F. W. Derrick, *The Oxidation and Corrosion of Zirconium and Its Alloys*, AERE-R2932 (August 1959).

<sup>28</sup>R. J. Davis, *Tabular Summary of Zircaloy-2 In-Pile Rocking Autoclave Corrosion Data*, ORNL CF-58-6-92 (June 18, 1958).

<sup>29</sup>R. J. Davis, *Tabular Summary of In-Pile Autoclave Solution Corrosion Data*, ORNL CF-59-9-75 (Sept. 24, 1959).

Table 1. Uranium Sorption in Scales and on Surfaces of Zircaloy-2 Specimens in Autoclave Experiments

Experiment Number	Initial Solution Composition, Approximate (m)			Exposure Temperature (°C)	Solution Power Density (w/cc)	Corrosion Rate at Steady State (mpy)	Uranium in Scale (wt %)	Uranium on Surface (μg/cm <sup>2</sup> )
	UO <sub>2</sub> SO <sub>4</sub>	CuSO <sub>4</sub>	H <sub>2</sub> SO <sub>4</sub>					
Z-1	0.17	0.01	0.04	280	10.3	11.8		
Z-2	0.17	0.01	0.04	280	10.8	13.1	3.4	
Z-15	0.17	0.04	0.04	280	11.8	13.6	1.3	
Z-17	0.17	0	0.04	280	1.4	3.1		
Z-101	0.17	0.04	0.04	280	8.2	10.6	1.1	
H-60	0.17	0.02	0.04	275	8.2	10.7		
Z-5	0.17	0.02	0	280	4.3	10.8	4.3	
Z-9	0.17	0.007	0	280	7.5	15.9	6.0	
Z-10 <sup>a</sup>	0.17	0.02	0	280	4.5	10.1	6.6	
Z-11 <sup>b</sup>	0.17	0.01	0	280	9.2	16.1	4.5	
Z-24	0.17	0.01	0	280	14.0	26.7	9.8	
Z-102	0.17	0.04	0	280	1.2	2.6	0.2	
Z-14	1.3	0.04	0.04	280	24.8		16	
Z-16	1.3	0.04	0.04	280	23.6	7.5	17	
Z-23	1.3	0.04	0.04	280	109	20.5		
Z-139 <sup>c</sup>	1.3	0.04	0.04	275	36	12.0		8
Z-18	0.04	0.06	0.04	280	4.9	9.9	2.6	
L53T-132 <sup>c</sup>	0.17	0.04	0.04	280	7.3		0.1	22
L52Z-136 <sup>c, d</sup>	0.17	0.040	0	270-330-270	11.4		3.3	8
					5.8			9
Z-8	0.18	0.02	0.05	250	11.4	5.4	2.3	
Z-20 <sup>c</sup>	0.17	0.04	0.04	250	9.3	7.5	6.3	
					18.6	8.7		
H-58	0.15	0.02	0	250	2.6	5.6		
					5.3	7.8		
H-59	0.31	0.04	0	250	11.9	6.1		
					7.1	4.9		
Z-3	0.17	0.02	0.45	250	3.7	6.9	0	

<sup>a</sup>Final in-pile exposure at 290°C.

<sup>b</sup>Final in-pile exposure at 232°C.

<sup>c</sup>The solvent for these solutions was D<sub>2</sub>O; the solvent for other solutions was H<sub>2</sub>O.

<sup>d</sup>Final in-pile exposure at 270°C.

16%, compared with an average of about 2% in the scales from specimens exposed in 0.17 *m* UO<sub>2</sub>SO<sub>4</sub> solutions but under otherwise comparable conditions. The amounts of scale uranium found in the few experiments with 0.04 *m* UO<sub>2</sub>SO<sub>4</sub> solutions are about the same as those in 0.17 *m* solutions. There is no indication that the amount of uranium in the scales changes appreciably with temperature in the range 230 to 290°C. The results of analyses for uranium on or in the underlying adherent film indicate that significant amounts of uranium may be sorbed by the film. They also indicate that the amount sorbed is not necessarily proportional to the amount found in the heavy scale.

The results of analyses for uranium on loop-core specimens in experiments L-2-17, L-2-19, and L-2-21 are summarized in Table 2, together with remarks regarding evidence for, or against, uranium sorption in these and in other loop experiments. The analytical results obtained in the L-2-17 experiment showed that appreciable amounts of uranium were sorbed on the specimen surfaces, and that the amount sorbed was less for the specimen exposed to the higher solution velocity. The observed corrosion rates for these specimens varied with velocity in the same direction. In experiment L-2-21, 1 to 6 μg/cm<sup>2</sup> of uranium were found on specimens exposed in the forward portion of the core and thus to the highest solution power densities. Other specimens in L-2-21 showed appreciable amounts of iron-bearing scale along with uranium, and the significance of these uranium results is obscure. Specimens from experiments L-2-19 and L-2-14, in which the solution contained Li<sub>2</sub>SO<sub>4</sub> and H<sub>2</sub>SO<sub>4</sub> additives, did not retain any significant amounts of sorbed uranium, and there was no apparent effect of solution velocity on the Zircaloy-2 corrosion rate.

The results of uranium analyses on the L-2-17 and L-2-19 specimens together with Zircaloy-2 corrosion results in these experiments are considered as evidence that the amount of uranium sorbed on Zircaloy-2 under irradiation decreases with increasing velocity of solution flow past the specimens. As shown in the remarks in Table 2, the observed effects of velocity on corrosion are employed in judging whether significant uranium sorption occurred on Zircaloy-2 specimens in other loop experiments where surface analyses for uranium were not carried out.

Uranium sorption on ZrO<sub>2</sub> from UO<sub>2</sub>SO<sub>4</sub> solutions at elevated temperatures has also been demonstrated in laboratory tests. The amounts sorbed per unit weight of oxide depend upon the thermal treatment received by the oxide prior to exposure, the solution composition, temperature, and probably other factors such as impurities in the oxide. These studies are in a preliminary stage, and the results will not be reviewed here except to note that, in general, the amount of uranium sorbed in these tests increased with increasing temperature.<sup>30,31</sup> Experimental data are unavailable for accurate estimations of the temperature effect on sorption within the temperature range employed in the in-pile corrosion tests. However, an idea of the temperature effect can be gained from the results of one experiment in which an increase of about 15% in the amount sorbed per gram of oxide was observed upon increasing the temperature from 250 to 280°C in a solution 0.12 *m* in UO<sub>2</sub>SO<sub>4</sub>

---

<sup>30</sup>B. O. Heston and G. H. Jenks, *HRP Quart. Progr. Rept. Oct. 31, 1958*, ORNL-2654, pp 180-83.

<sup>31</sup>J. C. Banter *et al.*, *HRP Quart. Progr. Rept. Jan. 31, 1960*, ORNL-2920, pp 78-81.

Table 2. Uranium Sorption on Surfaces of Zircaloy-2 Specimens Exposed in In-Pile Loop Cores

Experiment Number	Approximate Solution Composition (m)				Solvent	Temperature (°C)	Solution Velocity (fps)	Remarks
	UO <sub>2</sub> SO <sub>4</sub>	CuSO <sub>4</sub>	H <sub>2</sub> SO <sub>4</sub>	Li <sub>2</sub> SO <sub>4</sub>				
L-2-17 <sup>a</sup>	0.04	0.005	0.025		H <sub>2</sub> O	300	1-40	Two specimens exposed at solution velocities of 1 and 32 fps, respectively, showed uranium on the surface in the amounts of 21 and 5.5 μg/cm <sup>2</sup> and corrosion rates of 10.1 and 2.8 mpy respectively. A beneficial effect of increasing solution velocity noted with other specimens also.
L-2-21 <sup>b</sup>	0.17	0.022	0.04		D <sub>2</sub> O	280	1-18	1 to 6 μg/cm <sup>2</sup> of uranium on several specimens exposed to highest solution power densities. Uranium on other specimens indeterminate.
L-2-19 <sup>c</sup>	0.17	0.02	0.1	0.2	H <sub>2</sub> O	280	1-40	Several specimens exposed to velocity range 1 and 10-40 fps were examined and showed no significant retention of uranium. No beneficial effect of increased solution velocity on corrosion was observed.
L-2-14 <sup>d</sup>	0.17	0.15	0.4		H <sub>2</sub> O	280	1-40	Specimens appeared clean and there was no evidence of a velocity effect on corrosion. These results indicate negligible uranium sorption.
L-2-10 <sup>e</sup>	0.04	0.008	0.02		H <sub>2</sub> O	280	1-40	Evidence of beneficial effect of increasing solution velocity indicates significant uranium sorption at lower velocities.
L-2-15 <sup>f</sup>	0.17	0.015	0.03		H <sub>2</sub> O	280	1-40	Same as for L-2-10.
L-4-16 <sup>f</sup>	0.17	0.015	0.025		H <sub>2</sub> O	280	1-14	Same as for L-2-10.

<sup>a</sup>G. H. Jenks et al., HRP Quart. Progr. Rept. Jan. 31, 1958, ORNL-2561, pp 203-14.

<sup>b</sup>G. H. Jenks et al., HRP Quart. Progr. Rept. Oct. 31, 1958, ORNL-2654, pp 142-64.

<sup>c</sup>G. H. Jenks et al., HRP Quart. Progr. Rept. July 31, 1958, ORNL-2561, pp 214-26.

<sup>d</sup>G. H. Jenks et al., HRP Quart. Progr. Rept. Oct. 31, 1957, ORNL-2432, pp 107-19.

<sup>e</sup>G. H. Jenks et al., HRP Quart. Progr. Rept. Jan. 31, 1957, ORNL-2272, pp 104-8.

<sup>f</sup>G. H. Jenks et al., HRP Quart. Progr. Rept. July 31, 1957, ORNL-2379, pp 101-14.

and 0.02 *m* in H<sub>2</sub>SO<sub>4</sub>. Also, Lyon and Morgan<sup>32</sup> found an increase of at least 20% in the amount of uranium sorbed in passing from a temperature of 260 to 300°C in a solution in which the UO<sub>2</sub>SO<sub>4</sub> concentration was approximately 0.03 *m*.

As discussed in a previous report,<sup>33</sup> when uranium is sorbed near the surface during in-pile exposure, the intensity of fission-recoil irradiation of the surface may be considered as the sum of the contributions from uranium in solution and from the sorbed uranium:

$$P_c = P + kfU_w, \quad (11)$$

where  $P_c$  is the effective power density at the wall,  $P$  is the power density in solution,  $U_w$  is the amount of uranium sorbed per unit area,  $f$  is the neutron flux, and  $k$  is a constant, the value of which depends upon the precise location of the uranium. Since fission power density in solution is determined from the neutron flux and the uranium concentration in solution, Eq. (11) may be written as

$$P_c = P \left( 1 + n \frac{U_w}{U_s} \right), \quad (12)$$

where  $U_s$  is the uranium concentration in solution and  $n$  is a proportionality constant.

In practice, it is convenient to consider the effects of the uranium which is sorbed directly on the surface (hereafter called surface uranium) separately from those of the uranium sorbed in heavy scales (e.g., in the scales found in autoclave experiments). The surface uranium may have essentially zero absorber interposed between the uranium and the sites at which damage leading to corrosion acceleration occurs. On the other hand, the ZrO<sub>2</sub> in the nonprotective scales may absorb an appreciable fraction of the fission-recoil energy produced by the uranium in the scales as well as by that in the solution within fission-recoil range of the surface. Since the scales affect the solution contribution to the surface irradiation, the effects of the scale are represented by a term  $\gamma$  which replaces the term unity in Eq. (12):

$$P_c = P \left( \gamma + n \frac{U_w}{U_s} \right). \quad (13)$$

In this equation the term  $n(U_w/U_s)$  represents the effects of surface uranium. The value of  $\gamma$  may be greater or less than unity, depending upon the concentration of uranium in the scales. The factor  $\alpha$  is defined as

$$\alpha = \gamma + n \frac{U_w}{U_s}. \quad (14)$$

---

<sup>32</sup>R. N. Lyon and C. S. Morgan, *An Explanation of Pips and Pooops in the HRT*, ORNL HRP-59-191 (Oct. 22, 1959).

<sup>33</sup>G. H. Jenks, R. J. Davis, and J. R. McWherter, *HRP Quart. Progr. Rept. Oct. 31, 1957*, ORNL-2432, pp 116-19 and 120-26.

Some estimates of the values of  $n(U_w/U_s)$  and  $\gamma$  which might be expected under several of the experimental conditions employed in the in-pile corrosion tests are as follows:

**Uranium on the Surface.** – As shown in Table 2, the low-velocity specimens from experiment L-2-17 retained 21  $\mu\text{g}$  of uranium per  $\text{cm}^2$ . This is about the same amount of uranium as that contained in a layer of the 0.04  $m$  solution which is equal in thickness to the estimated range of 30  $\mu$  for fission recoils in the solution at the experiment temperature. It can be shown that about 25% of the fission recoils and about 10% of the fission-recoil energy originating in the solution within range of the wall are deposited in the wall. On the other hand, up to 50% of the fission recoils and fission-recoil energies formed in the fissioning of the surface uranium are deposited in the wall.<sup>34</sup> Hence, the estimated value of  $n(U_w/U_s)$  for the 21  $\mu\text{g}$  of surface uranium per  $\text{cm}^2$  is as high as 5, and if the value of  $\gamma$  is 1 (as expected in the absence of heavy scales) the estimated value of  $\alpha$  is 6. For the same amount of surface uranium in 0.17  $m$  or 1.3  $m$   $\text{UO}_2\text{SO}_4$  solutions, the estimated value of  $n(U_w/U_s)$  decreases from 5 to 1.2 or 0.15 respectively.

**Uranium in Scales.** – The simplest case to consider is that in which the  $\text{ZrO}_2$  scale is equal in thickness to the estimated range of about 6  $\text{mg}/\text{cm}^2$  for fission recoils in the scale. When this scale contains 1.5% uranium by weight and the uranium is uniformly distributed, the amount of uranium within range of the wall is about the same as that in a 30- $\mu$  layer of 0.17  $m$   $\text{UO}_2\text{SO}_4$  solution at 280°C, and the numbers and energies of fission recoils which originate in the scale and reach the walls are about the same as those which would prevail if the scale were replaced with the 0.17  $m$   $\text{UO}_2\text{SO}_4$  solution. The value of  $\gamma$  in Eq. (14) would then be 1. Similarly, lesser or greater amounts of scale uranium at the same solution concentration yield estimated  $\gamma$  values proportionately lesser or greater than 1. The estimated  $\gamma$  value for a given percentage of scale uranium changes with solution concentration and is inversely proportional to the solution concentration.

In practice, however, the scale does not reach the thickness of 6  $\text{mg}/\text{cm}^2$ . From geometrical considerations it can be shown that when the amount of uranium per unit of range in the scale is the same as that in solution, the scale does not alter the intensity of fission-recoil irradiation of the wall from that which would prevail in the absence of scale. The relationships between the relative contributions from the uranium in the scales and that in solutions for those cases in which the amounts of uranium per unit of range in the scale and in the solution differ and in which the scale thickness is less than the range have not been formulated. However, the qualitative effects of the scales are apparent for these cases.

#### 4. IN-PILE ZIRCALOY-2 CORROSION RESULTS

Three general types of data will be considered:

1. Sets of data obtained over a range of power densities at a given temperature and under

---

<sup>34</sup> See, for example, W. C. Yee, *A Study of the Effects of Fission Fragment Recoils on the Oxidation of Zirconium*, ORNL-2742, pp 81–88 (Apr. 29, 1960).

otherwise similar conditions so that the value of  $\alpha$  may be expected to remain constant within a set. Most of the data of this type were obtained in loop and autoclave experiments at 280°C, but some data for temperatures of 250 and 300°C are also available.

2. Data obtained in autoclave experiments which operated at 280°C and one or more other temperatures.

3. Data obtained in loop experiments which show an effect of solution velocity on corrosion.

#### 4.1 APPLICABILITY OF EQUATION TO CORROSION DATA

##### Value of $K$ and $K_1$ at 280°C

The 280°C data of type 1 are shown graphically in Fig. 1. In the graph, the reciprocal of the observed corrosion rate is plotted vs the reciprocal of the fission power density. The origin corresponds to an infinite corrosion rate and an infinite power density. The corrosion rate values employed are those based on total specimen area and radiation time. Solution compositions are given in Tables 1-3. All the autoclave experiments (lines *D* and *F* and points Z-16 and -23) were of the same type and employed vertically oriented autoclaves of Zircaloy-2.

The loop data shown by line *A* fall near a straight line which extrapolates to a value of 40 mpy at infinite power density. As discussed previously and noted in Table 2, there was probably a negligible effect from sorbed uranium on these specimens, and hence an  $\alpha$  value of 1 is assumed for these data. The calculated value of  $K_1$  is then 89 w/cc.

The results shown in lines *B-F* also fall near the straight lines which are drawn arbitrarily through the point on the ordinate determined by line *A*. Except for the autoclave experiments Z-16 and -23 using 1.3 *m* UO<sub>2</sub>SO<sub>4</sub> uranium sorption at the specimen surfaces very likely contributed to the effective power density at the surfaces in each of these experiments. However, in this treatment of the data, uranium sorption results only in a line of lower slope than expected for no significant sorption and has no effect on the value of  $K$ . Although lines *B-F* are arbitrarily drawn through a  $K$  value of 40 mpy, none of the results are considered to be inconsistent with this extrapolated value (the two points off line *F* will be discussed later). This apparent constancy of  $K$  for the different solutions was not predicted from the model, since one or more of the factors relating radiation damage with corrosion rate might be solution dependent. These results show that these factors are not affected to any large extent by solution composition.

The values of  $\alpha$  listed for lines *B-F* were calculated from the slopes of the lines using the value of  $K_1$  determined from the results of line *A*; that is, it was assumed, in accordance with the model, that the value of  $K_1$  does not change with solution composition. The relative values of  $\alpha$  thus determined appear reasonable as judged from the information available concerning the amounts of uranium held near specimen surfaces in the different experiments described in Sec 3.

Thus it may be estimated from comparisons with the results of analyses of the L-2-17 specimens that the low-velocity specimens in L-2-10 sorbed about 20  $\mu$ g of uranium per cm<sup>2</sup>. As shown previously (Sec 3), in the absence of any heavy scale the calculated  $\alpha$  value for this amount of

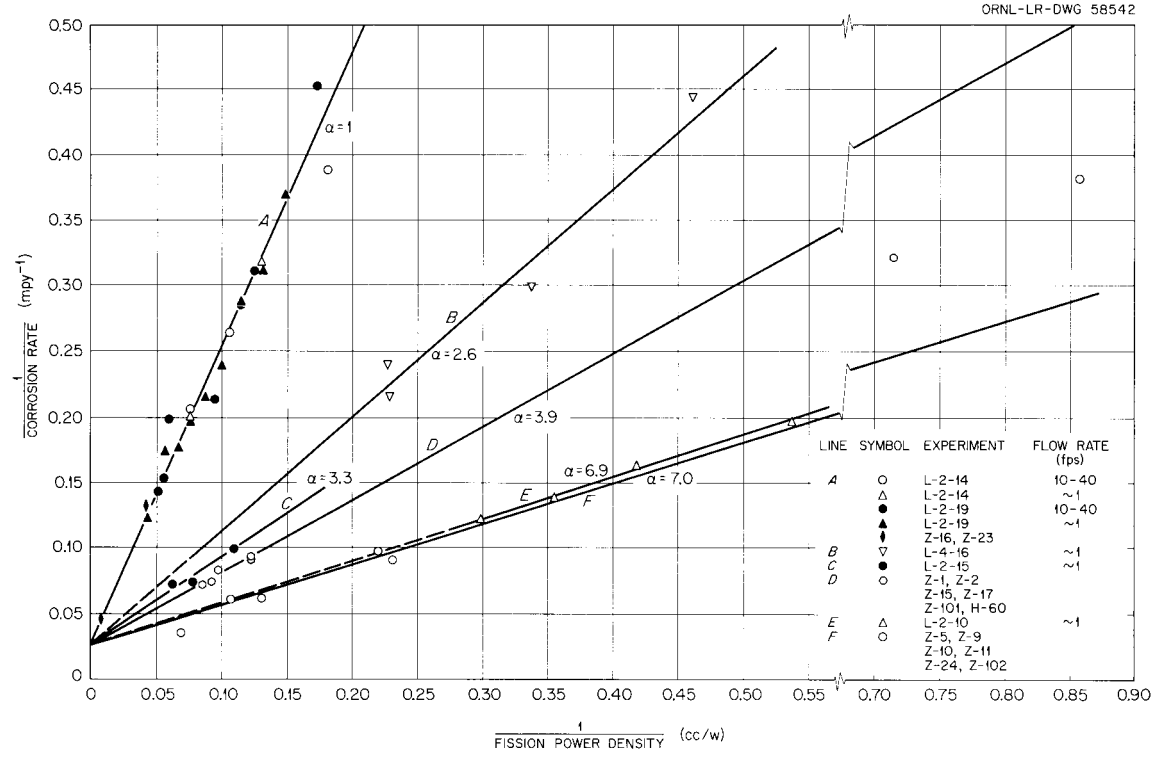


Fig. 1. Radiation Corrosion at 280°C from Loop and Autoclave Experiments. The calculated value of  $K_1$  from these data is 89 w/cc.

sorbed uranium and for a 0.04 m  $UO_2SO_4$  solution is about 6, based on fission-recoil energy deposition. On this basis the experimental value of 6.9 for  $\alpha$  for the L-2-10 low-velocity specimens appears reasonable. The difference between the values of  $\alpha$  obtained in the autoclave experiments which employed the 0.17 m  $UO_2SO_4$  solutions with and without excess  $H_2SO_4$  is in the direction expected from the difference between the amounts of uranium in the heavy scales (Table 1). However, the amounts found in the heavy scales are probably not sufficient to account fully for the observed values of  $\alpha$ . For example, scales with 1.3 or 1.1% uranium in 0.17 m  $UO_2SO_4$  solutions, as in the Z-15 and Z-101 scales, would not change the irradiation intensity at the wall appreciably from that prevailing in the absence of heavy scale (Sec 3). Thus, to account for the observed values of  $\alpha$  by means of sorbed uranium, the concentrations of uranium in the scales during exposure must have been greater than those found after exposure, or, alternatively, appreciable amounts of uranium must have been sorbed as surface uranium. Either explanation appears possible, although the latter is favored for these data, since, as shown by line C, an  $\alpha$  value of 3.3 was calculated for specimens exposed to low velocities in a loop experiment which employed a solution similar to those listed for line D. These loop specimens were free of heavy scale, and the  $\alpha$  value is explained by surface uranium in about the same amount as that required to account for the  $\alpha$  values for the data shown by line D.

It may be noted that the Z-24 and Z-102 points, which deviate appreciably from the line  $F$ , can also be qualitatively accounted for by the relative amounts of uranium found in these and in other comparable experiments shown in the figure. The scales from the other experiments contained 4 to 6% uranium, while those from Z-24 and Z-102 contained 9.8 and 0.2% respectively. The Z-24 point falls below the line and the Z-102 point above the line.

The indicated value of unity for  $\alpha$  in the 1.3  $m$   $UO_2SO_4$  autoclave experiments Z-16 and -23 is consistent with the available information on scale and surface uranium in these systems. The 16% uranium found in the scales is only slightly greater than the percentage (approximately 12%) for which little effect on the power density would be expected from the presence of the scale. Also, the amount of surface uranium indicated for Zircaloy-2 in these solutions (Table 1) would have a negligible effect on the irradiation intensity at the surface.

No information is available on the actual amount of uranium sorbed on the loop specimens represented by lines  $B$  and  $C$ . However, as noted in Table 2, the occurrence of a beneficial effect of velocity in these experiments indicates that appreciable uranium was sorbed on these low-velocity specimens.

These data are considered as strong support for the validity of an equation of the form of Eq. (2), and, assuming this validity, for the nondependence of the factors  $K_1$  and  $K$  on solution composition.

#### Value of $K$ at 250°C

The data from which the value of  $K$  at 250°C is estimated are shown in Fig. 2. For each of the experiments listed, the reactor operated at two different power levels during the in-pile exposure. Since no change other than the power level was made in a given experiment, it appears reasonable to assume that the value of  $\alpha$  did not change and that extrapolation of lines through the data yields fairly accurate values of  $K$ . The values thus obtained range from 9.4 to 12.5 mpy for these experiments, and the average value is 10.7 mpy. The values of  $K$  obtained at 280 and 300°C are given in Fig. 2 for comparison.

Other autoclave data obtained at 250°C are shown in Fig. 3. All the results shown were obtained in experiments which also were exposed at 280°C (the 280°C data have been shown in Fig. 1). It is apparent that these data are such that no accurate evaluation can be made of  $K$  from these data alone. However, they appear consistent with values of  $K$  determined from the data plotted in Fig. 2. It may be noted that the lower line is drawn through the point from experiment Z-11, and that points which fall above the line represent experiments in which the scale contained less uranium than Z-11 scales, and vice versa for those points which fall below the line.

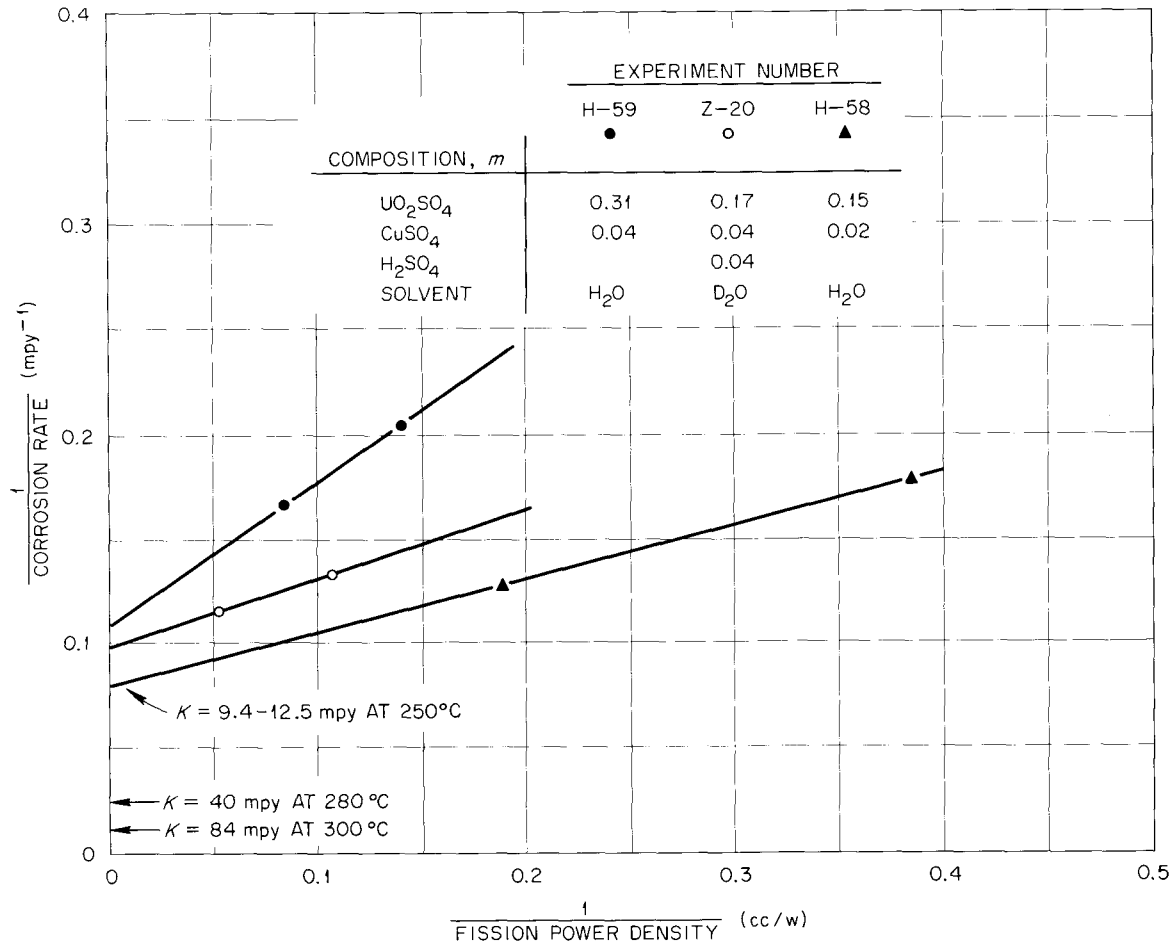


Fig. 2. Estimate of the Value of *K* from 250°C Autoclave Experiments.

### Value of *K* at 300°C

The data from which *K* at 300°C is estimated are shown in Fig. 4. These data were obtained with specimens exposed to a velocity of about 1 fps in loop experiment L-2-17. Because of the spread of the data and of the long extrapolation to infinite power density, the extrapolated value is considered quite uncertain, and values between 65 and 85 mpy appear consistent with the data.

### Relationship Between *K* and Temperature

As shown in Fig. 5, the *K* values determined at 250, 280, and 300°C fall near a straight line in a plot of the logarithm of *K* vs the reciprocal of the absolute temperature, indicating that an Arrhenius-type relationship is obeyed. The line is drawn such that it passes through the value of *K* at 280°C and within the range of values at 250 and 300°C indicated by the results of these temperatures. The line indicates *K* values at 250 and 300°C of 12 and 84 mpy respectively. The slope of the line corresponds to an activation energy of about 23 kcal/mole.

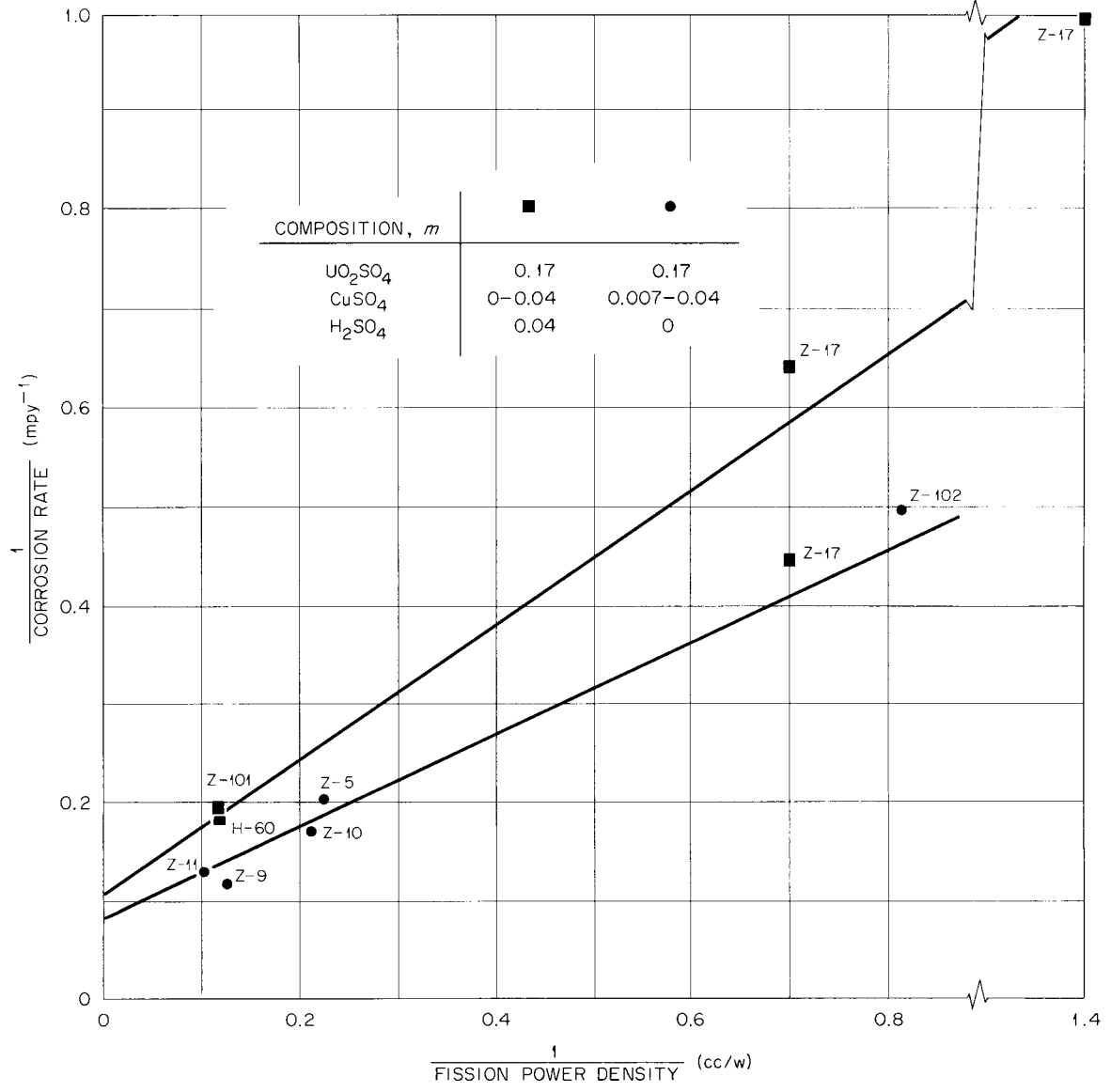


Fig. 3. Radiation Corrosion at 250°C from Autoclave Experiments.

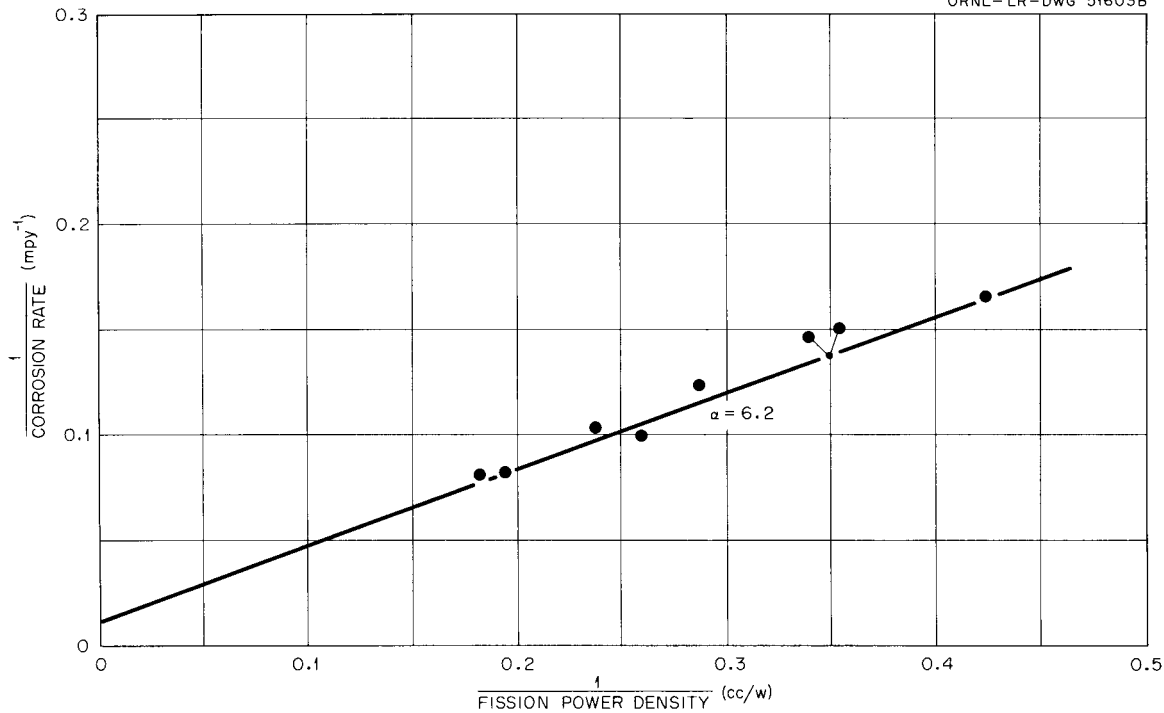


Fig. 4. Radiation Corrosion at 300°C from In-Pile Loop Experiment L-2-17. Solution composition: 0.04 *m* UO<sub>2</sub>SO<sub>4</sub>, 0.005 *m* CuSO<sub>4</sub>, 0.025 *m* H<sub>2</sub>SO<sub>4</sub>.

#### Other Values of $K_1$

The available experimental data are insufficient for direct determination of the values of  $K_1$  at temperatures other than 280°C. However,  $K_1$  values can be calculated from data of type 2 if it is assumed that the value of  $\alpha$  prevailing at the given temperature does not differ appreciably from that prevailing at 280°C in the same autoclave experiment, and also that the value of  $K$  at the given temperature is known.

The experimental data employed in the calculations, together with the calculated quantities, are listed in Table 3. The values for  $K$  were obtained from the lower line of Fig. 5. The approximate solution compositions for some of these experiments are listed under "Remarks" in Table 3. The compositions for the remainder of the experiments are included in Table 1. It should be noted that in each experiment the power density and  $\alpha$  values applying to the 280°C data were employed in the calculations of  $K_1$  values at the temperatures other than 280°C. The basis for this procedure can be explained by reference to Eq. (11). The term  $k/U_w$  may be considered as representative of the contribution of surface and scale uranium to the fission-recoil irradiation, and this does not change with temperature according to the assumption that  $U_w$  does not change appreciably with temperature. The amount of uranium in solution within range of the wall should be independent of temperature so that  $P$  also is temperature independent.

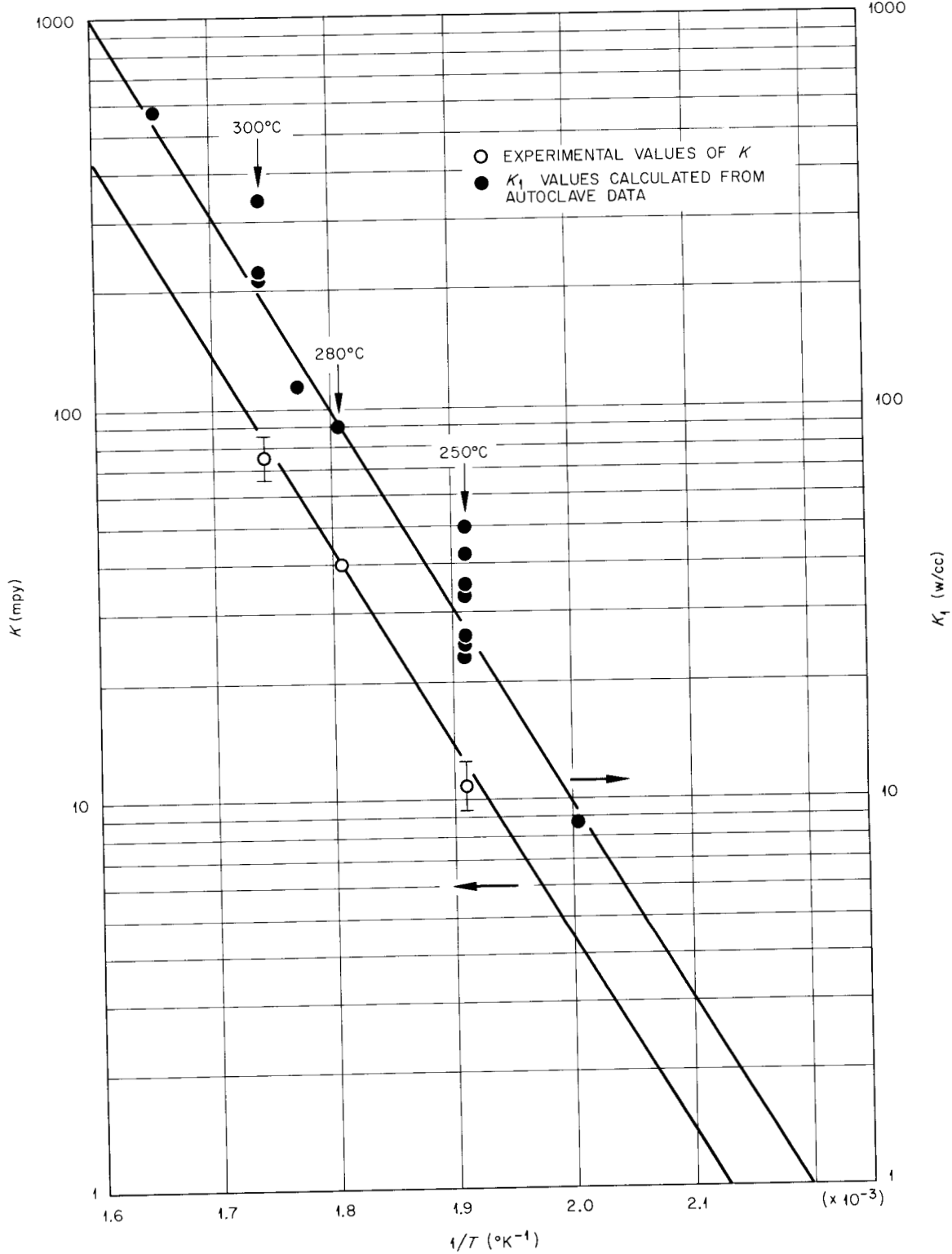


Fig. 5. Value of  $K$  and  $K_1$  as a Function of Temperature.

Table 3. Calculated Values of  $K_1$  in Autoclave Experiments

Experiment	Temperature <sup>a</sup> (°C)	Solution Power Density at 280°C (w/cc)	Corrosion Rate (mpy)	Calculated Value of $\alpha$ at 280°C	$K$ (mpy)	$K_1$ (w/cc)	Remarks
Z-19	280 <sup>b</sup>	17.1	24.2	7.97	40	89	0.17 m UO <sub>2</sub> SO <sub>4</sub> , no H <sub>2</sub> SO <sub>4</sub> , 0.0057 m MoO <sub>3</sub> added. <sup>c</sup>
	300	17.1	32.8	7.97	84	212	
Z-12	280 <sup>b</sup>	4.2	10.3	7.35	40	89	0.043 m UO <sub>2</sub> SO <sub>4</sub> , 0.02 m H <sub>2</sub> SO <sub>4</sub> (ref c).
	300	4.2	10.3	7.35	84	221	
Z-27	250	4.3	8.5	14.1	12	25	0.044 m UO <sub>2</sub> SO <sub>4</sub> , 0.031 m H <sub>2</sub> SO <sub>4</sub> (ref c). The observed rate at 300°C is anomalously low compared with the rates measured earlier at 280°C and 250°C. No explanation for this is apparent.
	280 <sup>b</sup>	4.3	16.2	14.1	40	89	
	330	4.3	21.5	14.1	227	579	
	300	4.3	12.8	14.1	84	337	
Z-10	225	4.5	3.1	6.68	4.0	8.7	
	250	4.5	5.7	6.68	12	33	
	280 <sup>b</sup>	4.5	10.1	6.68	40	89	
	290	4.5	12.2	6.68	58	113	
Z-11	250	9.2	7.6	6.52	12	35	The rate value measured at 232°C is equal to the estimated $K$ value for this temperature, and the value of $K_1$ is thus indeterminate. It may be noted that for the $K_1$ value to be in line with those measured at other temperatures, the value for the rate should be about 4.6 mpy. An error of about 1 mpy in the determination of the rate is considered possible.
	280 <sup>b</sup>	9.2	16.1	6.52	40	89	
	232	9.2	5.6	6.52	5.6	Indeterminate	
Z-101	250	8.2	5.3	3.93	12	41	
	280 <sup>b</sup>	8.2	10.6	3.93	40	89	
Z-16	250	23.6	6.1	(1)	12	23	Values of $\alpha$ at 280°C assumed to be unity (Fig. 1).
	280 <sup>b</sup>	23.6	7.5	(1)	40	89	
Z-102	250	1.2	2.2	5.17	12	26	
	280 <sup>b</sup>	1.2	2.6	5.17	40	89	
Z-5	250	4.3	4.8	7.66	12	49	
	280 <sup>b</sup>	4.3	10.8	7.66	40	89	
Z-9	250	7.5	8.3	7.85	12	26	
	280 <sup>b</sup>	7.5	15.9	7.85	40	89	

<sup>a</sup>For each experiment, the order in which the exposures to the different temperatures was carried out is the same as the order of listing.

<sup>b</sup>Values of  $K$  and  $K_1$  at 280°C assumed to be the same as those found in other 280°C experiments.

<sup>c</sup>R. J. Davis, *Tabular Summary of Zircaloy-2 In-Pile Rocking Autoclave Corrosion Data*, ORNL CF-58-6-92 (June 18, 1958).

The calculated  $K_1$  values in Table 3 are shown graphically as the upper line in Fig. 5. Although there is appreciable scatter among the several calculated points at 250°C, it appears that the  $K_1$  values over the range of temperature from 235 to 330°C are adequately represented by the straight line drawn parallel to the  $K$  line. The level of the line was determined by averaging the ratio of  $K_1/K$  for each of the points, including the ratio 2.23 at 280°C with a weight of 10 but excluding the 300°C point from experiment Z-27. The weight at 280°C was assigned on the basis that the value of the ratio at this temperature is well established by the data presented in this section and that this ratio was employed in calculating each of the other values. The average ratio of  $K_1/K$  thus determined is 2.3 w cc<sup>-1</sup> mpy<sup>-1</sup>. It may be noted that this value for the ratio  $K_1/K$  is also indicated by the results obtained with the low-velocity specimens in loop experiment L-2-17 and plotted in Fig. 4. Assuming that the value of  $\alpha$  prevailing for these specimens was about 6, as calculated from the amount of uranium found on the surface of the one specimen examined (Sec 3), the calculated value of the ratio  $K_1/K$  is about 2.3 when the value of  $K$  is 84 mpy.

The accuracy of the  $K_1$  values calculated as described is, of course, dependent upon the accuracy of the assumption that uranium sorption does not change appreciably with temperature, and that the proper value of  $K$  at the given temperature was chosen. As discussed in Sec 3, the results of analyses of scale from in-pile experiments exposed at different temperatures do not show any significant effects of temperature on the amount of uranium in the scales. The results of laboratory experiments show that the uranium sorption on ZrO<sub>2</sub> increases with increasing temperature, but that the amount of increase within the temperature range under consideration may be small, that is, 20 to 25% for a 40°C increase in temperature. Such a change in uranium sorption in the experiments considered above could be responsible for some of the variations in the calculated values of  $K_1$  at 250°C. These variations, however, could also be accounted for by small differences between the assumed value of  $K$  at 250°C and the true value prevailing in a given experiment. For example, a decrease in the assumed value of  $K$  from 12 to 10 mpy in experiment Z-101 (Table 3) would result in a calculated value of 27 rather than 41 for  $K_1$ . As shown in Fig. 2, such differences in the value of  $K$  for different experiments do exist. It can be noted that similar absolute differences in the value of  $K$  at temperatures of 280°C and above would have a negligible effect on the calculated values of  $K_1$  at these temperatures.

#### 4.2 EFFECT OF SOLUTION VELOCITY ON CORROSION

In experiments L-2-15, L-4-16, L-2-10, and L-2-17 (Table 2) there were beneficial effects when the solution velocity was increased. The results obtained at low solution velocities (approximately 1 fps) for each of these experiments have been described. The results obtained at velocities of 10 to 40 fps in these experiments will be reviewed. Results obtained at velocities of approximately 1 to 40 fps in the 280°C experiment L-2-21 and those obtained at velocities of 10 to 40 fps in the earlier experiments at 250°C will also be reviewed.

In each of the 280 and 300°C experiments to be considered, coupon-type specimens were exposed to velocities of about 1 fps in the core annulus and at velocities of about 10 to 40 fps in venturi-shaped channel holders with three angles. The velocities of about 10 fps prevailed at the entrance and exit ends, and the highest velocities were near the middle of the holder. In every case, the entrance end was exposed to the highest solution power densities and the exit end to the lowest. The holders were shaped such that three different angles were included between different specimens and the walls. From the front to the rear these angles were about  $-3^{\circ}40'$ ,  $-1^{\circ}5'$ , and  $3^{\circ}40'$ , where the minus sign indicates convergent flow.

The method of mounting specimens in the channel holders was such that an appreciable fraction of a specimen surface was covered by the holder and by adjacent specimens (about 35% covered). These covered surfaces were not sealed and thus were probably exposed to a thin layer of essentially static solution at the same time that the remainder of a specimen was exposed to an appreciable solution velocity. The fraction of the surface of annulus specimens which was covered was about the same as that for the channel specimens in each experiment except L-2-10, where about 90% of the surface was exposed. Channel specimens of the same or similar types were employed in the 250°C loop experiments. No annulus-specimen data of the type obtained in the 280 and 300°C experiments are available for these 250°C experiments.

The results obtained with channel and annulus specimens in loop experiments L-2-15, L-4-16, L-2-10, and L-2-17 are shown in Figs. 6-9, respectively, as plots of  $1/R$  vs  $1/P$ .

Results obtained with channel and annulus specimens in the 280°C experiment L-2-21 are shown in Fig. 10. As mentioned in Table 2, the presence of iron-bearing scale on many of these specimens renders the interpretation of these results uncertain, but they are included for completeness of the presentation.

Results obtained with channel specimens in the earlier 250°C loop experiments are illustrated in Fig. 11. The results obtained in some autoclave experiments previously described are included for reference. Also, the results obtained in a 235°C loop experiment are included to illustrate the lower rates observed at the lower temperature.

As discussed in Sec 3, the difference between the corrosion rates of channel and annulus specimens exposed at similar power densities in a given experiment is very likely a result of differences between the amounts of uranium sorbed on specimens exposed to the different solution velocities prevailing in the channel and annulus, with the amount sorbed being less at the higher velocities. Analytical results obtained in experiment L-2-17 showed that the amount of uranium retained on an annulus specimen was greater than the amount retained by a channel specimen exposed at a similar power density but at a velocity of about 32 fps. Also, in experiment L-2-19, in which uranium sorption on channel and annulus specimens was negligible, there was no significant difference between the rates observed for specimens exposed in the channel and annulus.

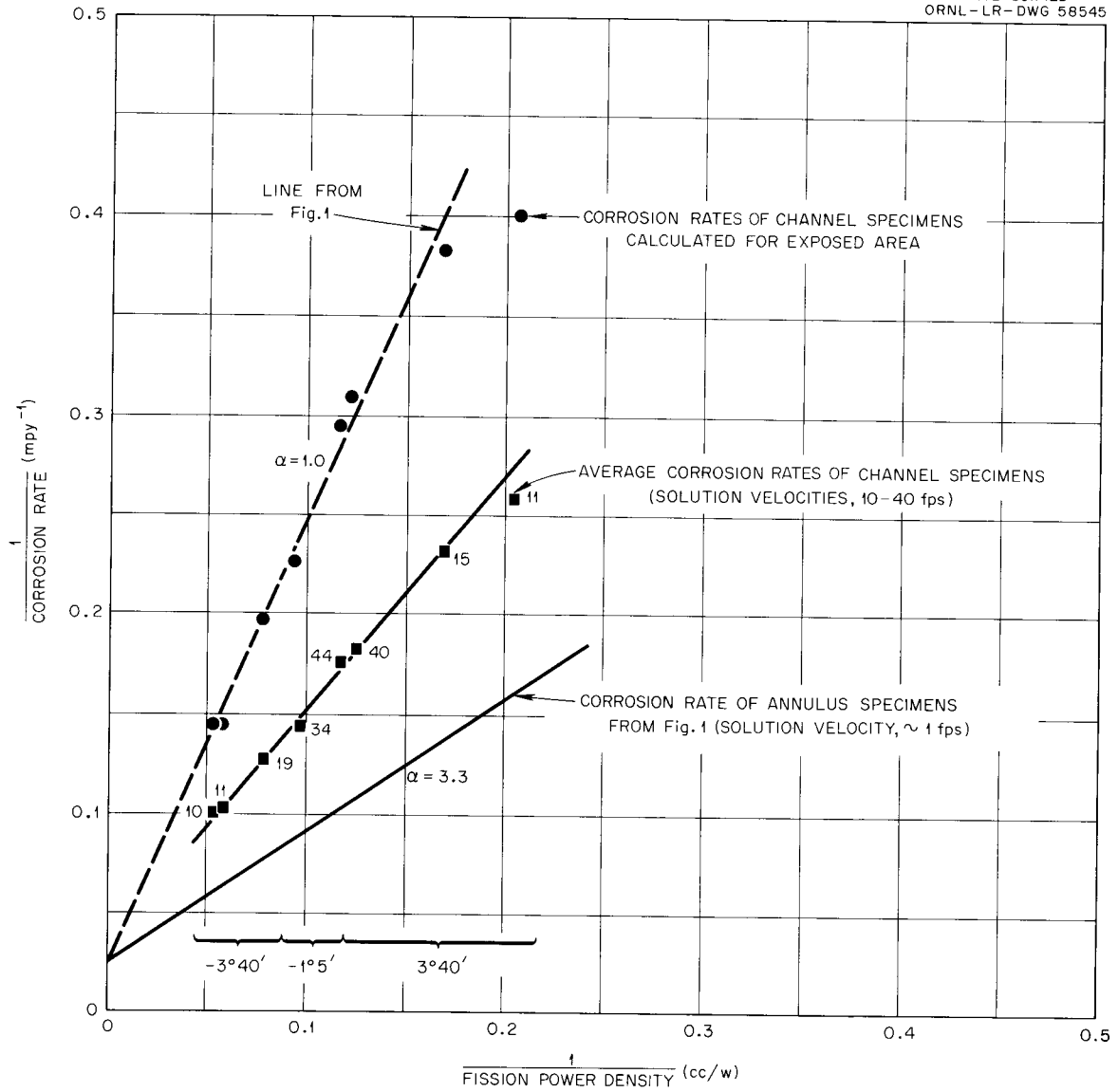


Fig. 6. Radiation Corrosion at 280°C from In-Pile Loop Experiment L-2-15. Numbers by points are average solution velocities in fps. Braces indicate included angle for channel specimens. Solution composition: 0.17 m UO<sub>2</sub>SO<sub>4</sub>, 0.015 m CuSO<sub>4</sub>, 0.03 m H<sub>2</sub>SO<sub>4</sub>.

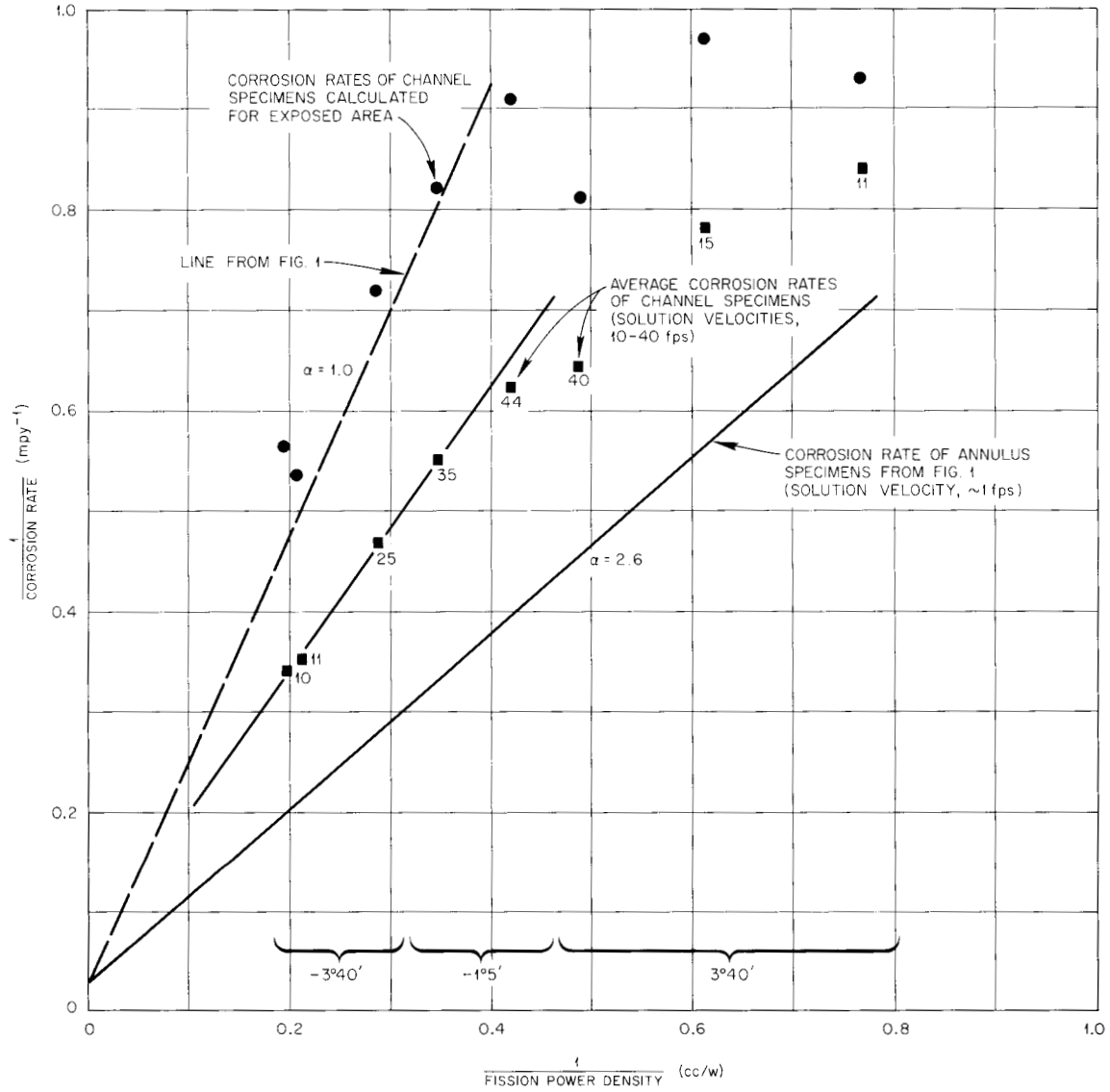


Fig. 7. Radiation Corrosion at 280°C from In-Pile Loop Experiment L-4-16. Numbers by points are average solution velocities in fps. Braces indicate included angle for channel specimens. Solution composition: 0.17 m UO<sub>2</sub>SO<sub>4</sub>, 0.015 m CuSO<sub>4</sub>, 0.025 m H<sub>2</sub>SO<sub>4</sub>.

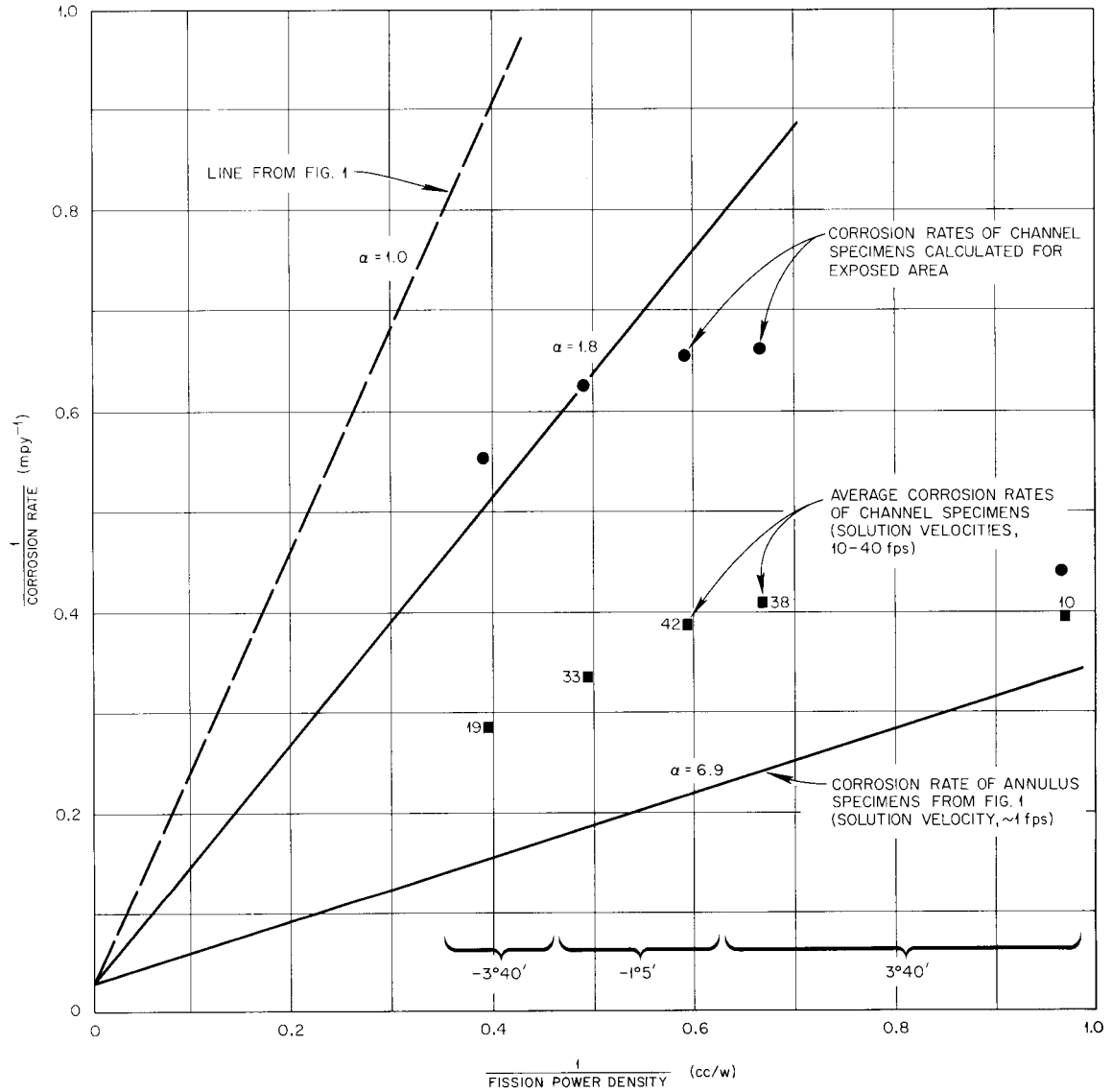


Fig. 8. Radiation Corrosion at 280°C from In-Pile Loop Experiment L-2-10. Numbers by points are average solution velocities in fps. Braces indicate included angle for channel specimens. Solution composition: 0.04 m UO<sub>2</sub>SO<sub>4</sub>, 0.0075 m CuSO<sub>4</sub>, 0.02 m H<sub>2</sub>SO<sub>4</sub>.

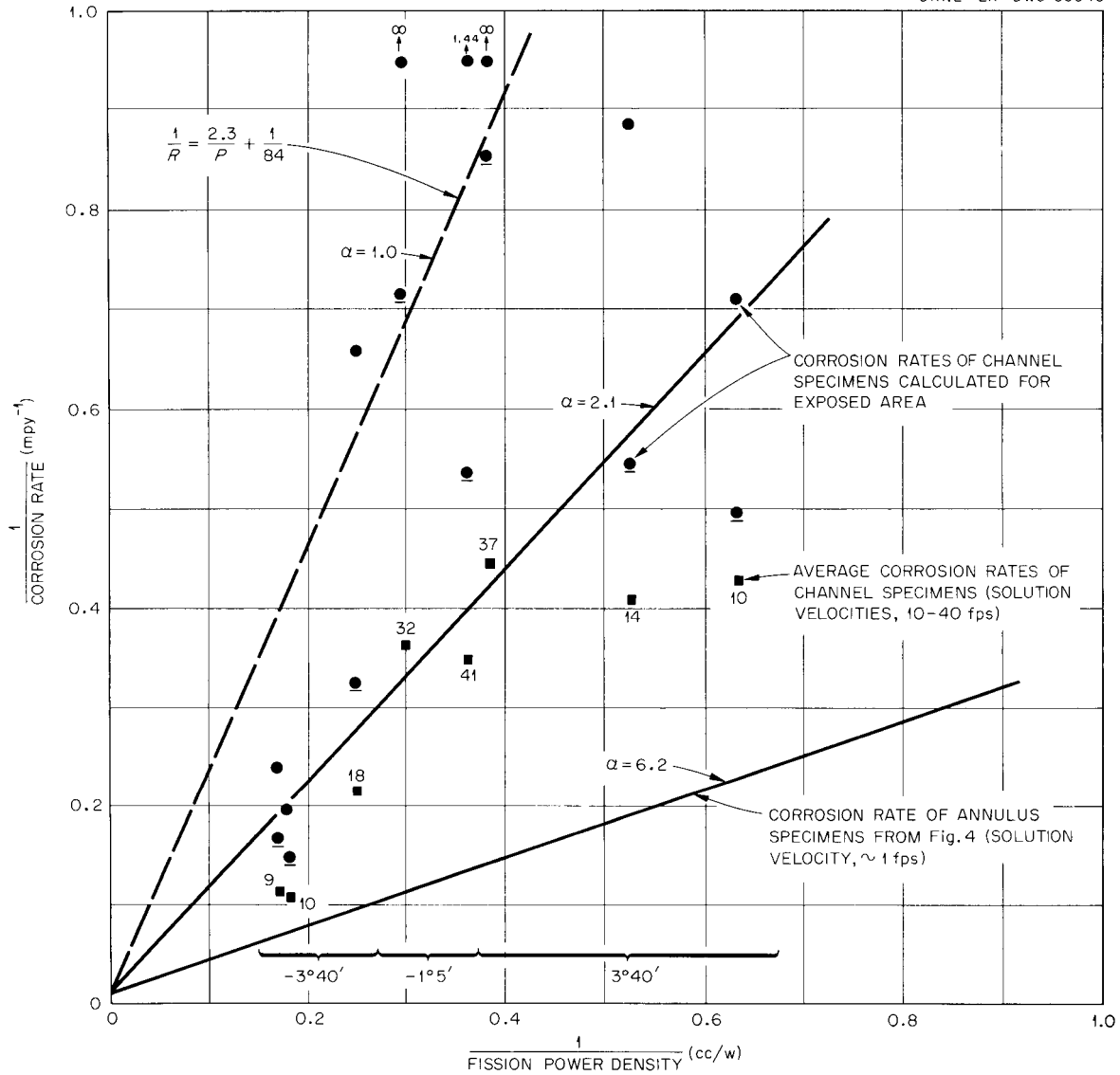


Fig. 9. Radiation Corrosion at 300°C from In-Pile Loop Experiment L-2-17. Numbers by points are average solution velocities in fps. Braces indicate included angle for channel specimens. Solution composition: 0.04 m UO<sub>2</sub>SO<sub>4</sub>, 0.005 m CuSO<sub>4</sub>, 0.025 m H<sub>2</sub>SO<sub>4</sub>.

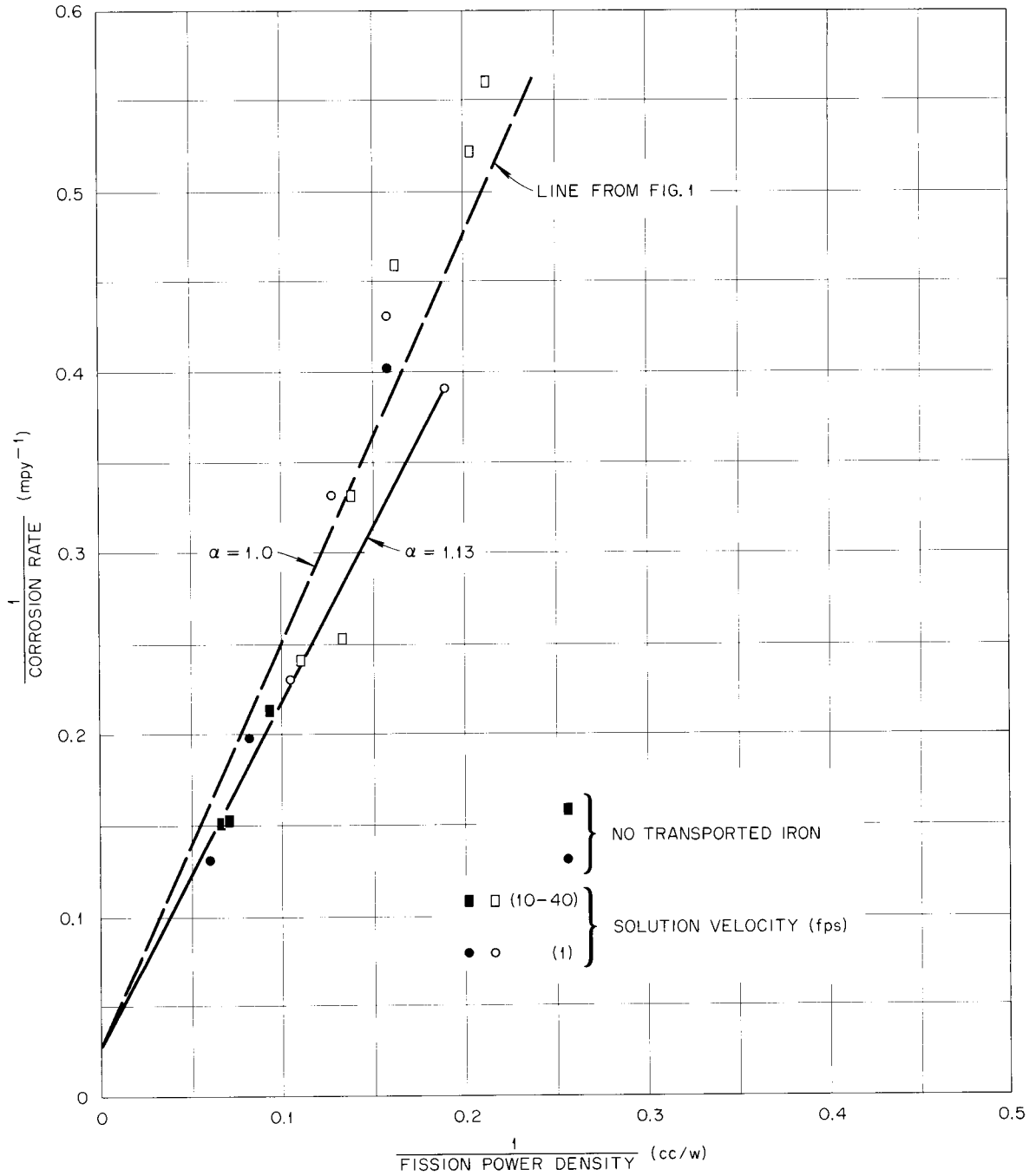
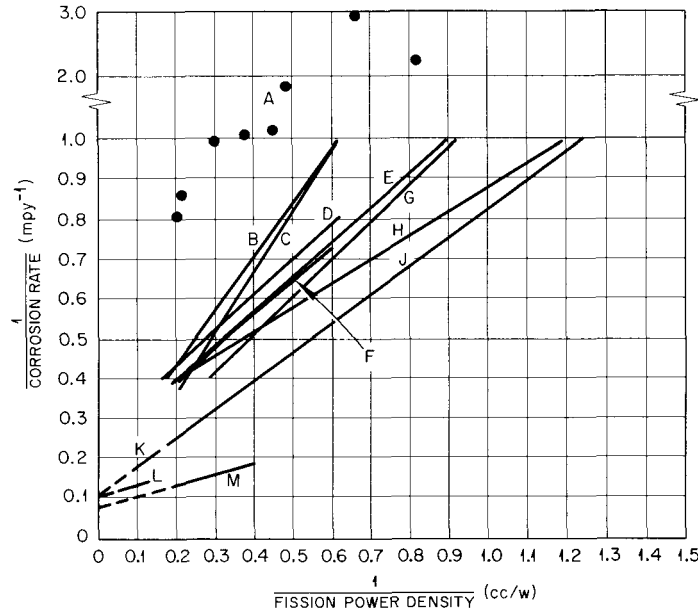


Fig. 10. Radiation Corrosion at 280°C from In-Pile Loop Experiment L-2-21. Solution composition: 0.17 m UO<sub>2</sub>SO<sub>4</sub>, 0.02 m CuSO<sub>4</sub>, 0.04 m H<sub>2</sub>SO<sub>4</sub>.



EXPERIMENTS REPRESENTED

Symbol	Experiment Number	Solution Composition (m) Approx.			
		UO <sub>2</sub> SO <sub>4</sub>	CuSO <sub>4</sub>	H <sub>2</sub> SO <sub>4</sub>	Solvent
Loops (Solution Velocity, 10-40 fps)					
A <sup>a,b</sup>	L-4-18	0.15	0.06	0.02	D <sub>2</sub> O
B <sup>c</sup>	EE	0.17	0.03	0.008	H <sub>2</sub> O
C <sup>d,e</sup>	L-4-12	0.17	0.03	0.04	H <sub>2</sub> O
D <sup>f,g</sup>	L-4-13	0.17	0.03	0.02	D <sub>2</sub> O
E <sup>h</sup>	FF	0.17	0.03	0.04	H <sub>2</sub> O
F <sup>h</sup>	GG				
G <sup>h,i</sup>	L-4-11				
H <sup>h</sup>	L-4-8				
Autoclaves (Solution Velocity, << 1 fps)					
J <sup>j</sup>	Z-101, 8, 17, and H-60	0.17	0-0.04	0.04	H <sub>2</sub> O
K <sup>i,k</sup>	H-59	0.31	0.04	0	H <sub>2</sub> O
L <sup>i,k</sup>	Z-20	0.15	0.036	0.036	D <sub>2</sub> O
M <sup>i,k</sup>	H-58	0.15	0.02	0	H <sub>2</sub> O

<sup>a</sup>Experiment at 235°C.  
<sup>b</sup>Jenks *et al.*, ORNL-2561, pp 203-14.  
<sup>c</sup>Jenks *et al.*, ORNL-2004, pp 123-53.  
<sup>d</sup>Loop core of Ti, remainder of loop of 347 SS.  
<sup>e</sup>Jenks *et al.*, ORNL-2222, pp 101-6.  
<sup>f</sup>Crystal-bar zirconium.  
<sup>g</sup>Jenks *et al.*, ORNL-2331, pp 113-18.  
<sup>h</sup>Baker and Jenks, ORNL-2042; McWherter and Baker, ORNL-2152; Jenks *et al.*, ORNL-1895, pp 99-117; Jenks *et al.*, ORNL-1943, pp 109-25.  
<sup>i</sup>Straight channel holders, solution velocity, ~ 10 fps.  
<sup>j</sup>Davis, ORNL CF-58-6-92.  
<sup>k</sup>The reactor operated at two different power levels during each of these experiments.

Fig. 11. Radiation Corrosion at 235 and 250°C from In-Pile Loop Experiments.

The detailed interpretations and evaluations of the results shown in Figs. 6–11 are dependent upon (1) estimates of the corrosion rates on covered surfaces, (2) considerations of the graphical interpretations of corrosion rate values which are averages of two different rates – one for the exposed and another for the covered surfaces, and (3) considerations of possible influences of channel angle on the relative effects on uranium sorption of a given average solution velocity. In the following paragraphs, these three factors are considered separately and a discussion then presented of the experimental result which is based on these considerations.

#### **Covered Surfaces of Channel Specimens**

An appreciable fraction of the surface of a given channel specimen was exposed to essentially static solution while the remaining surface was exposed to an appreciable solution velocity. Although the layer of solution over a covered surface was very thin, it has appeared likely that under some conditions these surfaces would sorb more uranium and thus corrode at higher rates than the exposed surfaces. Direct experimental evidence for a difference in the rates between covered and exposed surfaces has been obtained in a recent experiment not discussed here. The results of this experiment indicate that the rates on the covered surfaces were probably near those expected in stagnant, bulk solution.

In view of the results of this recent experiment, it is reasonable to assume that the corrosion rates on the covered surfaces in a given experiment were not less than those indicated for low-velocity annulus specimens in the same experiment and at the same given power densities. For each of the experiments in which annulus-specimen data are available, an estimation of the corrosion rates on the exposed surfaces of channel specimens has been made by assuming this equality between the rates on covered surfaces and on the annulus specimens. These resulting calculated rates are shown Figs. 6–9.

In the case of the L-2-17 data in Fig. 9, it appears that the exposed-area rates calculated in this manner are too low, since the calculated rates for the specimens exposed to 32 and 37 fps are about zero ( $1/R = \infty$ ), and the point for the 41-fps specimen also falls far above the line for  $\alpha = 1$ . For these data, another set of exposed-area rates have been calculated, assuming that the corrosion rates on the covered surfaces were less than those for the annulus specimens by the amount required (40% less) in order that the calculated rates for the 32- and 37-fps specimens fall near the line for  $\alpha = 1$ . The rates thus calculated are plotted in Fig. 9 and are identified by underlined points.

#### **Graphical Interpretation of the Averages of Rates on Exposed and Covered Surfaces**

Corrosion rates of specimens as usually presented are calculated from the results of weight-loss measurement, assuming that the corrosion penetration indicated by the weight loss is uniform over the entire surface of a specimen. When this is not the case because of different values of  $\alpha$  on different portions of a specimen, the relationship between the average corrosion rate and the power density which can be formulated from equations of the form of Eq. (2) is not

the simple  $1/R$  vs  $1/P$  relationship. By graphical methods, it has been found that for the conditions which probably prevailed in the experiments under consideration, the average-rate values fall near straight lines in  $1/R$  vs  $1/P$  plots when one  $\alpha$  value prevails for the exposed surfaces of a given set of specimens and another, higher, value prevails for the covered surfaces. However, under certain conditions, the apparent value of  $K$  determined by extrapolation of a line through the data points is less than the value assumed in the calculation of the average rates. Thus, in the case of the L-2-15 results,  $\alpha$  values of 1 and 4 were assumed for the exposed and covered surfaces of the channel specimens, respectively, and a  $K$  value of 40 mpy was also assumed. In a  $1/R$  vs  $1/P$  plot the calculated average-rate points fell near a straight line which extrapolated to 30 mpy rather than 40 mpy on the ordinate. Using the same values of  $\alpha$ , a  $K$  value of 10 mpy, and the power-density range covered in the 250°C experiments, the calculated average-rate values fall near a straight line which extrapolates to a value of about 7 mpy on the ordinate. For the L-2-10 and L-2-17 annulus data, an assumed difference of a factor of 2 between the  $\alpha$  values for the exposed and covered surfaces led to extrapolated  $K$  values which were not appreciably different from those assumed in the calculations.

### Influence of Channel Angle

It is known that the ratio of the solution velocity at the wall to that in the center of channels such as those employed depends upon the included angle, and decreases with increasing values of the angle.<sup>35</sup> The removal of uranium or other material from a specimen surface probably depends upon the velocity near the surface, and thus it is expected that the beneficial effects of a given average solution velocity decrease with increasing value of the angle.

### Discussion of Experimental Results for Velocity Effects on Corrosion

In experiment L-2-15 (Fig. 6) the calculated values for the rates on exposed surfaces fall near the line for  $\alpha = 1$ , with the exception of the point at the lowest power density and highest included angle. These results are considered as evidence that the value of  $\alpha$  on the exposed surfaces was near unity at velocities of 10 fps and above and for the included angles of  $-3^\circ 40'$  and  $-1^\circ 5'$ . The low point (high rate) at the lowest power density is probably a result of the lower wall velocities expected at the high included angle. At the 10-fps average velocity and at the angle of  $+3^\circ 40'$  which prevailed for this specimen, some uranium may have been retained on the exposed surface of the specimen, while none was retained at higher velocities and/or at smaller angles. These results, in general, are considered as evidence that the assumption of equal rates for the covered surfaces and for the low-velocity annulus specimens is valid.

---

<sup>35</sup>Hermann Schlichting, *Boundary Layer Theory*, English translation, p 463, McGraw-Hill, New York, 1955.

In experiment L-4-16 (Fig. 7) the calculated rates for the exposed surfaces of the channel specimens exposed to convergent flow also fall near the line for  $\alpha = 1$ . The points for the remainder of the specimens which were exposed to divergent flow fall below the  $\alpha = 1$  line. The results for the convergent-flow specimens provide further evidence for the validity of the assumption of equality between the rates for the covered surfaces and for annulus specimens. They also confirm the results obtained in L-2-15, which indicate the absence of significant amounts of sorbed uranium at velocities of 10 fps and above in convergent flow. The results for the other specimens in this L-4-16 experiment probably reflect a decreased beneficial effect of velocity in the divergent flow.

The calculated rates for the exposed surfaces of channel specimens in experiment L-2-10 (Fig. 8) are greater than those expected for  $\alpha = 1$ , even at the low included angle of  $-3^{\circ}40'$  and at the average solution velocity of 19 fps. This may be a true result in this dilute uranium solution (0.04 *m* vs 0.17 *m* in L-2-15 and L-4-16). However, it may also be assumed that the  $\alpha$  value for this low-angle specimen should be unity and that the covered-area rates were greater by a small amount (approximately 20%) than those indicated by the annulus specimens. This question cannot be resolved with the available information. The data for other specimens in this experiment indicate that significant amounts of uranium were sorbed on the exposed surfaces, since the calculated rates for all these specimens fall below a line drawn through the point for the low-angle specimen. These results are again attributed to a decreasing beneficial effect of solution velocity as the included angle increases.

In experiment L-2-17 (Fig. 9) the results for the average corrosion rates of channel specimens and the calculated values for the rates on the exposed surfaces differ from those obtained in the L-2-10 experiment discussed above in that there is no apparent effect of included angle on the beneficial effect at a given average solution velocity. Also, as mentioned previously, the corrosion rates on covered surfaces of the three high-velocity (32 to 41 fps) specimens were probably less than the rates found on annulus specimens at similar power densities. The latter effect might be due to peculiarities of the specimens and holders and of the properties of the solution at 300°C resulting in some solution flow over portions of the covered surfaces of the high-velocity specimens. Similar effects might or might not occur with the lower velocity specimens, and, in recognition of this uncertainty, two calculated rate values are presented for each specimen, as discussed previously. These calculated values are considered as the probable maximum and minimum values for the rates on the exposed surfaces of the lower velocity specimens.

Most of the specimens in experiment L-2-21 (Fig. 10) retained appreciable amounts of iron-bearing scale, and those specimens which were free of this scale exhibited only small amounts of uranium. The results for the scale-free specimens appear to be in line with those expected for values of  $K_1$  and  $K$  determined in other 280°C experiments and for a small value of  $\alpha$  as indicated by the small amounts of retained uranium. The presence of the scales on the other specimens renders the interpretations of the weight and sorbed-uranium measurements uncertain for

those specimens. However, all the points fall near the  $\alpha = 1$  line, and the relatively low rates indicated for the lower-power-density specimens may be due to errors in the weights or from  $\gamma$  values less than unity resulting from the presence of the scales.

The explanation for the low uranium sorption and the correspondingly low  $\alpha$  value in this experiment is unknown.

As is evident in Fig. 11, the 250°C loop results fall near straight lines in  $1/R$  vs  $1/P$  plots, but for most of the experiments, the lines extrapolate to rate values at infinite power density which are less than the rates of 10 to 12 mpy established by the autoclave results. As mentioned in the discussions above, it can be shown that an extrapolation to an apparently low rate value occurs when average corrosion-rate values are employed and when the  $\alpha$  value prevailing for the exposed surfaces of a given set of specimens is appreciably less than that for the covered surfaces. This factor is probably a partial explanation for the deviation of the extrapolated values from the 10- to 12-mpy rate. Another factor of probable importance is that the included angle in the channel decreased in passing from the high- to the low-power-density ends of the channel, and hence the effective velocity at a given average solution velocity probably decreased with decreasing power density. This effect would tend to result in relatively high rates at the lower power densities.

The spread of the low-corrosion-rate results obtained in the 235°C experiments is such that no conclusions can be drawn from a line through the data.

In general the results obtained with the specimens exposed to high solution velocities in the various experiments considered above show that solution flow has a beneficial effect on corrosion and that this effect can be attributed in all cases to a reduction or elimination of uranium sorption due to the solution flow. There is no evidence for a deleterious effect of velocity on corrosion up to the highest velocities employed (approximately 40 to 50 fps). The results obtained with the L-2-15 and L-4-16 experiments at 280°C tend to confirm the relationship between corrosion rate and power density deduced from other data as described in Sec 4.1. The results obtained with the experiments other than L-2-15 and L-4-16 are such that they do not provide direct tests of the relationships. However, these data appear consistent throughout with the previously determined relationships.

The indicated magnitudes of the beneficial effects of solution velocity are such that for 0.17  $m$   $UO_2SO_4$  solutions and convergent-type flow, uranium sorption is negligible at average velocities of 10 fps and higher, whereas it can be appreciable at velocities of about 1 fps. In the 0.04  $m$   $UO_2SO_4$  solutions, the results indicate that the  $\alpha$  value is between unity (negligible uranium sorption) and 1.7 at the average solution velocities of about 18 fps and above and for the channel angle of  $-3^\circ 40'$ . The  $\alpha$  values at the average velocity of 10 fps and for the  $-3^\circ 40'$  angle probably are between 2 and 3.

The facts — that uranium sorption at Zircaloy-2 surfaces may be reduced or eliminated as a result of some action associated with solution flow and that the flow has no apparent adverse

effects on corrosion – suggest that the sorbed uranium is not incorporated in the protective film. Instead, it probably is sorbed on nonprotective oxide of rather high surface area (porous oxide) which tends to adhere to the protective oxide, but which is removed at sufficiently high shear stress between the solution and the surface.

## 5. CONCLUSIONS

1. The results of the correlations of the many in-pile experimental results of Zircaloy-2 corrosion at the exposure temperature of 280°C indicate that a general relationship between corrosion rate and solution power density is obeyed within the power-density range tested (up to 110 w/cc). This relationship can be expressed as

$$1/R = K_1/KP\alpha + 1/K, \quad (2)$$

where  $R$  is the corrosion rate, mpy;  $P$  is the solution power density, w/cc;  $\alpha$  is the factor by which the effective power density at a corroding surface is greater than that in solution due to uranium sorption on the surface; and  $K_1$  and  $K$  are constants the values of which are essentially independent of solution composition. In the case of  $K_1$ , this solution independence was expected on the basis of the model from which Eq. (2) was derived. The solution independence of  $K$  was not predicted, but it is not inconsistent with the model.

2. On the basis of the reasonable assumption that a relationship between corrosion rate and power density of the general form of Eq. (2) is obeyed at the other temperatures as well as at 280°C, values of  $K$  at 250 and 300°C were estimated. The values thus estimated together with the value determined from the 280°C data indicate that an Arrhenius-type relationship prevails between the value of  $K$  and temperature and that the value of  $K$  is expressed by

$$K = 4.44 \times 10^{10} \exp(-22,900/RT), \quad (15)$$

where  $K$  has the units mpy and  $R$  is the gas constant.

3. The results of further correlations of data available in the temperature range 225 to 330°C, in which it is assumed that the value of  $\alpha$  in a given autoclave system did not change appreciably with changing temperature, indicate that the ratio  $K_1/K$  does not change appreciably with temperature. The ratio has the value of about  $2.3 \text{ w cc}^{-1} \text{ mpy}^{-1}$ , so that the corrosion-rate–power-density relationship in this temperature range can be represented by

$$1/R = 2.3/P\alpha + 1/K, \quad (16)$$

where  $K$  is given by Eq. (15).

4. The data available for the radiation-induced corrosion of Zircaloy-2 coupon specimens exposed in-pile to high-velocity solutions in tapered-channel holders can be reasonably interpreted on the basis that the relationship between corrosion rate and power density for these specimens is expressed by Eq. (16) and that the flow of solution past a specimen surface tends to minimize

uranium sorption and thus the value of  $\alpha$  prevailing for the surface. There is no evidence in these data for any adverse effect of the solution velocity on corrosion.

In general, for a given solution composition, the indicated amount of uranium sorbed on the channel specimens depends upon the average solution velocity and upon the included angle in the channel at the specimens. This result suggests that the shear stress between the solution and the surface is an important factor in the determination of the beneficial effect of velocity. No quantitative correlations between shear stresses and uranium sorption were attempted.

The various results obtained with the high-velocity specimens indicate that sorbed uranium is not incorporated in the protective oxide, but instead is sorbed on nonprotective oxide of high surface area which adheres to the protective oxide but which can be removed at sufficiently high shear stresses between the solution and the wall.

Some quantitative results obtained with the high-velocity specimens are: (1) In aqueous solutions containing 0.17 *m* UO<sub>2</sub>SO<sub>4</sub> and 0.02–0.03 *m* H<sub>2</sub>SO<sub>4</sub> at 280°C, the  $\alpha$  values were in the range 2.5 to 3.5 for solution velocities of about 1 fps. For specimens exposed to convergent-type flow ( $-3^{\circ}40'$  and  $-1^{\circ}5'$ ) and to average velocities of 10 fps and above, the  $\alpha$  value was unity. (2) In aqueous solutions containing 0.04 *m* UO<sub>2</sub>SO<sub>4</sub> and 0.02–0.025 *m* H<sub>2</sub>SO<sub>4</sub> at either 280 or 300°C, the  $\alpha$  values were in the range 6 to 7 for solution velocities of about 1 fps. The probable  $\alpha$  values at velocities of 10 and 18 fps and at the included angle of  $-3^{\circ}40'$  were 2 to 3 and 1 to 1.7 respectively. (3) In aqueous solutions at 280°C, containing 0.17 *m* UO<sub>2</sub>SO<sub>4</sub>, 0.15 *m* CuSO<sub>4</sub>, and 0.4 *m* H<sub>2</sub>SO<sub>4</sub> in one case and 0.17 *m* UO<sub>2</sub>SO<sub>4</sub>, 0.02 *m* CuSO<sub>4</sub>, 0.1 *m* H<sub>2</sub>SO<sub>4</sub>, and 0.2 *m* Li<sub>2</sub>SO<sub>4</sub> in another case, the values were unity at all velocities and angles (to the maximum velocity of about 40 fps).

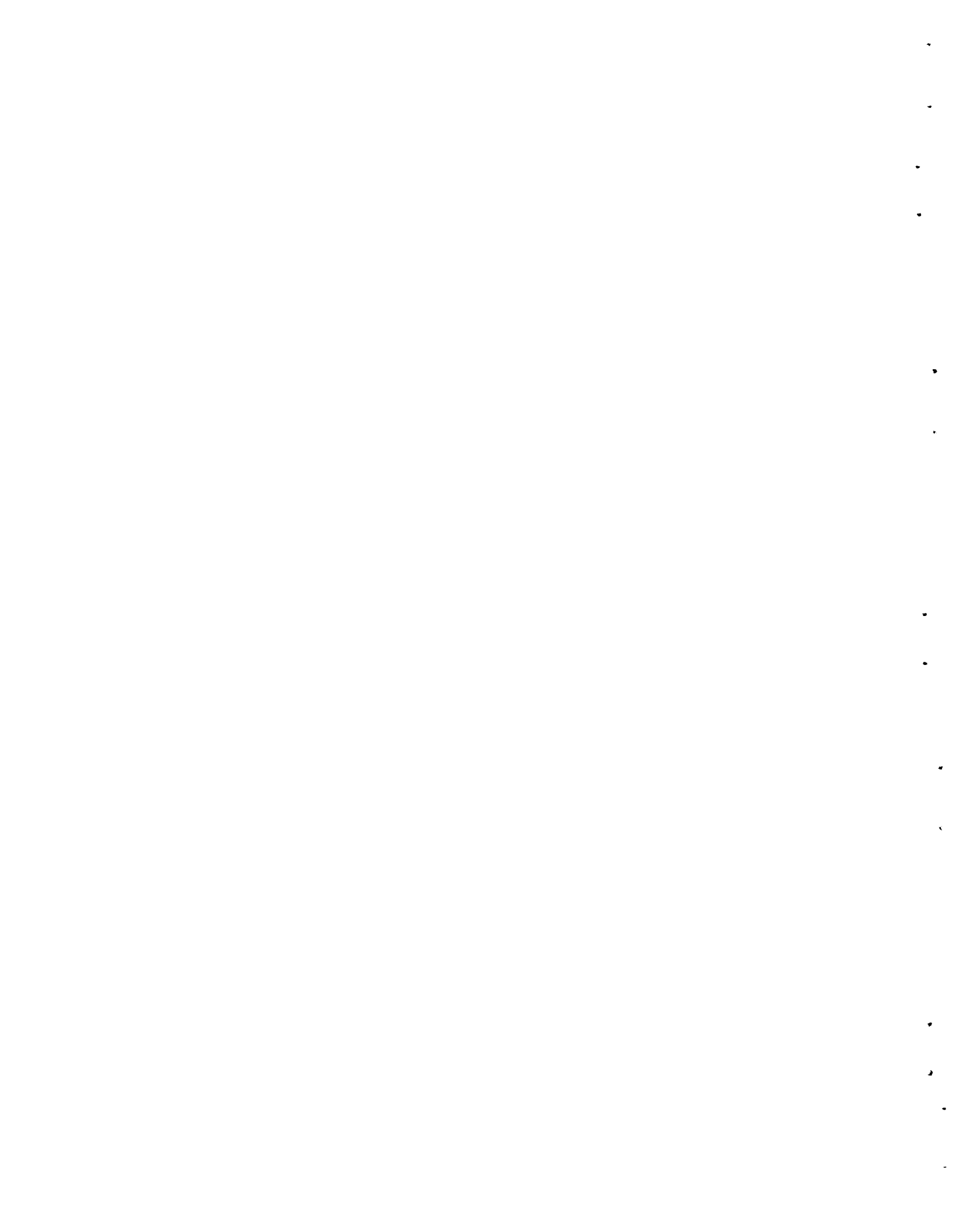
## APPENDIX

### POSSIBLE SIGNIFICANCE OF TEMPERATURE INDEPENDENCE OF THE RATIO $K_1/K$

The results of correlations of the Zircaloy-2 radiation-corrosion data indicate that the ratio  $K_1/K$  does not change appreciably with temperature in the range investigated (225 to 330°C), although the value of  $K$  does change in this range. There is also some evidence, not described in this report, that the value of the ratio  $K_1/K$  for crystal-bar zirconium at a given temperature is the same as that for Zircaloy-2, although the values of  $K$  for the two materials differ by a factor of about 2. A possible interpretation of these observations is that an annealing of the radiation defects occurs at a rate directly proportional to the corrosion rate and that thermal annealing of the defects is negligible. In this case the final term in Eq. (4) can be written as  $K'aN$ , where  $K'$  represents the number of defects removed per corrosion event, and the ratio of  $K_1/K$  in Eq. (2) reduces to the ratio of  $K'/K''$ , which might be essentially independent of temperature and of solution composition.

The mechanism by which an annealing directly proportional to the corrosion might occur can be visualized as one in which the radiation defects in the metal near the metal-oxide interface

react in the corrosion process and are thus removed. However, the over-all process by which a steady-state concentration of defects results at the surface of the metal from the formation and radiation annealing of defects at appreciable depths and from corrosion annealing of defects at the surface of the metal is by no means clear. It appears likely that for the steady state to occur as specified in Eq. (5), with corrosion annealing rather than thermal annealing, it would be necessary for defects to diffuse readily to the surface from appreciable depths in the metal (a few tenths of a micron or more). Further considerations of the possibilities of such rapid diffusion of defects near the metal-oxide interface as well as of other processes or revisions of the model which might explain the constancy of the ratio will be required before this particular corrosion-annealing mechanism can be accepted.



INTERNAL DISTRIBUTION

1. HRP Director's Office  
Rm. 259, Bldg. 9204-1
2. G. M. Adamson, Jr.
3. A. L. Bacarella
4. C. F. Baes
5. J. E. Baker
6. J. M. Baker
7. J. C. Banter
8. S. E. Beall
9. A. M. Billings
10. D. S. Billington
11. F. F. Blankenship
12. A. L. Boch
13. E. G. Bohlmann
14. S. E. Bolt
15. G. E. Boyd
16. R. B. Briggs
17. J. R. Brown
18. W. D. Burch
19. G. H. Cartledge
20. J. V. Cathcart
21. C. E. Center
22. R. H. Chapman
23. R. A. Charpie
24. E. L. Compere
25. L. T. Corbin
26. F. L. Culler
27. D. G. Davis
28. R. J. Davis
29. O. C. Dean
30. V. A. DeCarlo
31. D. M. Eissenberg
32. J. L. English
33. C. Feldman
34. D. E. Ferguson
35. J. H. Frye
36. C. H. Gabbard
37. W. R. Gall
38. J. P. Gill
39. J. C. Griess
40. W. R. Grimes
41. P. A. Haas
42. P. H. Harley
43. P. N. Haubenreich
44. J. W. Hill
45. E. C. Hise
46. H. W. Hoffman
47. G. H. Jenks
48. R. G. Jordan (Y-12)
49. P. R. Kasten
50. G. W. Keilholtz
51. M. T. Kelley
52. M. J. Kelly
53. J. A. Lane
54. C. G. Lawson
55. R. A. Lorenz
56. R. N. Lyon
57. M. I. Lundin
58. W. D. Manly
59. W. L. Marshall
60. J. P. McBride
61. R. E. McDonald
62. H. F. McDuffie
63. H. G. MacPherson
64. J. R. McWherter
65. R. E. Meyer
66. R. L. Moore
67. C. S. Morgan
68. J. P. Murray (K-25)
69. A. R. Olsen
70. F. N. Peebles
71. M. L. Picklesimer
72. F. A. Posey
73. J. L. Redford
74. D. M. Richardson
75. H. C. Savage
76. C. H. Secoy
77. M. D. Silverman
78. M. J. Skinner
79. B. A. Soldano
80. I. Spiewak
81. J. A. Swartout
82. F. J. Sweeton
83. A. Taboada
84. E. H. Taylor
85. P. F. Thomason
86. M. Tobias
87. W. E. Unger

- 88. K. S. Warren
- 89. G. M. Watson
- 90. A. M. Weinberg
- 91. S. H. Wheeler
- 92. J. C. White
- 93. C. E. Winters
- 94. W. C. Yee
- 95. F. W. Young
- 96. H. Zeldes
- 97. H. E. Zittel
- 98-99. Reactor Division Library
- 100-101. Central Research Library
- 102-103. ORNL - Y-12 Technical Library,  
Document Reference Section
- 104-122. Laboratory Records Department
- 123. Laboratory Records, ORNL R.C.
- 124. F. T. Gucker (consultant)
- 125. F. Daniels (consultant)
- 126. F. T. Miles (consultant)

#### EXTERNAL DISTRIBUTION

- 127. D. H. Groelsema, AEC, Washington
- 128. F. P. Self, AEC, Oak Ridge
- 129. M. E. Wadsworth, University of Utah
- 130. Division of Research and Development, AEC, ORO
- 131-722. Given distribution as shown in TID-4500 (16th ed.) under Chemistry category  
(75 copies - OTS)